FINAL TECHNICAL REPORT

submitted to

OFFICE OF NAVAL RESEARCH

DEPARTMENT OF THE NAVY

under

CONTRACT NO. N00014-84-C-0464

PROJECT NO. NR 083-702/4-06-84 (420)

A STUDY TO DETERMINE THE MERIT OF OCEAN BOREHOLE SYSTEMS FOR ACOUSTIC DETECTION

by

F. Duennebier
C. McCreery
D. Harris
R. Cessaro
C. Fisher
P. Anderson

July 31, 1985

HAWAII APPLIED RESEARCH, INCORPORATED
P. O. BOX 61592
HONOLULU, HAWAII 96822

TABLE OF CONTENTS

INTRODUCTION

This report presents results of analysis of active and passive seismic signals and background noise recorded on an ocean subbottom (OSS-IV) and ocean bottom seismometers (OBS), for the purpose of determining their relative merits for acoustic detection. Results from OSS-IV noise and signal propagation studies document the increase in signal fidelity and signal-to-noise ratio obtained at this site. Attenuation analysis of short line data indicates that loss at OSS-IV is more than expected from spherical spreading, but the low noise level of the instrument makes it sensitive to sources in the ocean for long ranges.

SUMMARY REPORT

Data obtained by an ocean borehole experiment at 44°N, 160°E has been analyzed in order to evaluate the detection capability of a borehole seismic system as compared to an ocean bottom system. Absolute noise levels for the complete duration of the 64-day experiment were also determined, indicating the borehole site to be one of the quietest sites in the world. Source spectrograms show the passage of ships, whales, and storms near the site. Selected sections of data have been reduced and sent to Rondout for directivity analysis and source identification. A paper entitled "Geo-Acoustic Noise Levels in a Deep Ocean Borehole" has been presented and published (Appendix E). A preliminary preprint of a paper entitled "Orientation of Horizontal Ocean Bottom Seismic Sensors from Explosive Data" (resulting from a parallel HIG study) is included as pertinent to this study (Appendix F).

Task I. - Evaluation of the detection capability of the borehole seismic system.

OSS-IV is one of the quietest seismic stations in the world at frequencies between 4 and 15 Hz. Noise levels of $10^{-12} m^2/Hz$ are observed above 4 Hz. Noise at frequencies above 5 Hz appears to be caused by system noise during quiet periods, but dominated by storm generated noise at other times. Shipping, whales, and earthquakes also add to the noise. Equivalent acoustic noise varies between 60 and 70 dB re 1 μPa, about 10 dB quieter than the ocean. Signals generated in the ocean can be detected at long distances, with propagation loss on the order of 120 dB (referenced to a source level at 1 m) at 100 km. Earthquake signals are observed about once per hour with S/N ratios and fidelity considerably improved over those

amplitude decreases slightly less than a factor of two with every reflection from the ocean bottom at pre-critical angle.

Task II. - Source Identification

Data reduction and transmission of 257 hours of selected data required for directivity study has been completed. A directivity study of shot data has provided the sensitivity azimuths of the OSS-IV horizontal geophones. This was accomplished by analyzing first arrival particle motions from 20 explosives fired at various azimuths and ranges. As a result of this study, the geophone azimuths were determined to ±1.5 degrees. The azimuth to impulsive sources can be determined to ±6 degrees. While conducting this study, it was found that in order to satisfy geometric requirements of the navigation and azimuthal data, Hole 581C had to be moved approximately 500 m to the west of the ship's position while drilling. Appendix F is a preliminary preprint of the paper describing this analysis.

Task III. - Evaluation of the desireability of a shallow-water borehole experiment.

A shallow-water experiment appears to be justified and practical within reasonable cost. Preliminary propagation models for the shallow water case provide a general view of the propagation mechanisms in shallow water. These results predict that much of the energy propagating up slope is not lost, but is transmitted in and along the ocean floor. If this proves to be the case, then a borehole seismometer may well be a valuable tool for shallow-water detection, particularly at low frequencies. While geoacoustic modeling appears to be unreliable at present, results suggest that shallow water low-frequency energy may be best detected in boreholes. At shallow

depths and low frequencies, the sediments act as part of the water column wave guide. By installing geophones in boreholes, excessive noise levels generated by low shear velocities in the sediments, Scholte waves, and ocean waves can be avoided. Careful experiments in shallow-water areas of interest, under varied conditions, can determine whether the possible increases in directivity and signal-to-noise ratio can be realized.

OSSIV: NOISE LEVELS, NOISE SOURCES, AND SIGNAL TO NOISE

F. Duennebier
C. McCreery
D. Harris
R. Cessaro
C. Fisher
P. Anderson

Progress Report Submitted to:

The Office of Naval Research

Contract N00014-84-C-0464
Project No. NR 083-702/4-06-84 (420)

July 25, 1984

Abstract: OSSIV is one of the quietest seismic stations in the world at frequencies between 4 and 15 Hz. Noise levels of $10^{-12} m^2/Hz$ are observed above 4 Hz. Noise at frequencies above 5 Hz appears to be caused by system noise during quiet periods, but dominated by storms at other times. Shipping, whales and earthquakes also add to the noise. The equivalent acoustic noise level varies between 60 and 70 dB re 1μPa, about 10 dB quieter than the ocean. Signals generated in the ocean can be heard out to long distances, with propagation loss on the order of 120 dB (referenced to a source level at 1 m) at 100 km. Signals generated from earthquakes are observed about once per hour with S/N ratios and fidelity considerably improved over those obtained from OBS's. Bottom loss measurements indicate that acoustic signal amplitudes decrease by slightly less than a factor of two with every reflection from the ocean bottom at pre-critical angles.

I. Introduction. The quantization of noise, signal-to-noise ratios (S/N), signal propagation, and noise sources is of primary importance in this experiment. The question, "Do increases in signal fidelity and S/N down the hole versus sensors in the ocean or on the ocean floor justify the cost of emplacing seismic sensors in ocean drill holes?," must be answered before more experiments are seriously considered. In this report we present results from OSSIV noise and signal propagation studies that document the increase in fidelity and S/N obtained at this site. We believe that the results justify further experiments.

Other experiments have obtained ocean acoustic and seismic noise levels (Urick, 1981; Nichols, 1981; Carter et al., 1984; Adair et al., in press) with acoustic levels at 10 Hz commonly between 80 and 90 dB re 1 Pa/Hz, and seismic levels on the ocean floor as low as 20 pm/Hz , but normally above 100 pm/Hz . Carter et al. found that equivalent noise levels near 100 pm/Hz were found on an OBS and OSSII when an impedance correction was applied to the OSS data. OSSII was emplaced in soft sediment 194 m below the OBS. The MSS 1981 experiment achieved noise levels of about 500 pm/Hz at 2 Hz but did not obtain data above 2 Hz (Adair et al., in press). Data from the MSS experiment on DSDP Leg 91 is being analyzed by J. Orcutt and others at Scripps Inst. of Oceanography.

When comparing noise levels, it is important to take into account the elastic properties of the material in which the noise is measured. Since energy is proportional to the density and wave velocity of the material (ρc, the acoustic impedance), particle motion amplitudes will vary as the square root of the impedance (Carter et al., 1984). Thus, noise levels in dense, high velocity material will be deceptively lower than those in low density,

low velocity material. When comparing different systems in different media, a correction should be applied.

This report is divided into several sections dealing with the noise and propagation effects observed at the OSSIV site. First, absolute noise levels obtained early in the experiment are compared with an OBS for the same time period, and the temporal variation of noise over the 64-day analog recording period is discussed. In this section the origin and characteristics of the noise and the known sources are discussed. In the second section, S/N is evaluated for both earthquakes and acoustic sources in the ocean and propagation loss for acoustic sources is evaluated. Lastly, preliminary conclusions are drawn concerning the value of ocean borehole seismic/acoustic sensors.

II. Absolute Noise Levels, Temporal Variation of Noise, and Noise Sources. Absolute noise level measurements were obtained from two OBS's and the OSS during the emplacement of OSSIV. Sample noise spectra are shown in Figure 1. The OSS vertical component noise level is more than 20 dB quieter than the OBS levels over most of the frequency band. Note the similarity between the ISOBS (Byrne et al., 1983) spectrum and the OSS spectrum. Both show similar spectral peaks and shapes, although the OSS spectrum has a better S/N ratio for the peak at 20 Hz (generated by the nearby D/V GLOMAR CHALLENGER) than the ISOBS. The OSU OBS spectrum was taken at a few hours away from the other two, and does not show the same structure. To correct for the difference in impedance between the basalt in the borehole (ρ = 2.3 gm/cm^3, c = 3.0 km/sec) and the sediment under the OBS (ρ = 1.3 gm/cm^3, c = 1.6 km/sec) the OSS curve should be raised by 5.2 dB.

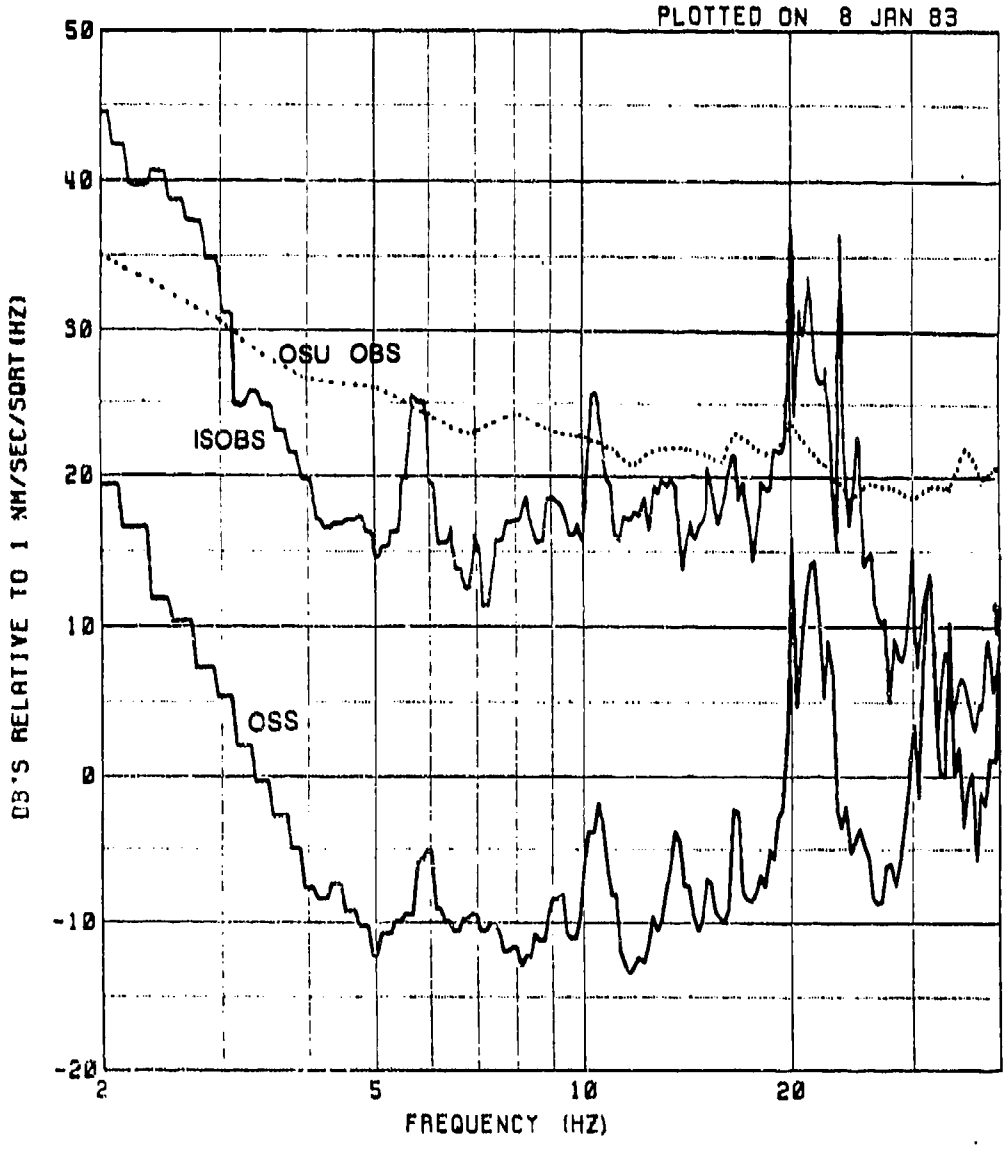

Figure 1. Noise level comparisons. This figure shows the comparison between the OSS vertical geophone and noise on two ocean bottom seismometer vertical geophones during the emplacement phase of OSSIV. Spectra were taken on Day 254, 1982 at 0815Z for a 30-second period.

A more striking difference in noise levels is seen between the OSS and the ISOBS horizontal components (Figure 2). In this case, the difference in noise levels is nearly 30 dB across the spectrum. The OSS horizontal noise levels are about the same as the vertical levels, but the ISOBS horizontal is about 10 dB noisier than the vertical levels. This extra noise is probably caused by trapping of horizontally polarized energy in the shear wave guide at the top of the sediments.

During recovery of the recording package nine months after emplacement of OSSIV, noise levels were again measured and found to be about 10 dB lower than measured during emplacement. This quieting probably represents a combination of filling in of the drill hole and better weather. In Figure 3, the OSS noise levels (during a relatively quiet period) are compared with the Lajitas continental borehole station in Texas (Herren, 1982). The OSSIV noise level increases at about 20 dB/octave with decreasing frequency below 6 Hz and levels out above 6 Hz. The continental noise levels increase at about 12 dB/octave below 20 Hz before leveling off. In both cases, the leveling of the noise at high frequencies is likely to be caused by system noise rather than seismic noise. The difference at the low frequency end of the spectrum is most likely the result of coupling of ocean movement above the OSS into the motion of the ocean floor. If this is the case, this noise level will change with ocean swell and storms, and decrease at longer periods where the OSS geophones are not sensitive.

Temporal changes in noise level were measured during a continuous 64-day period from September 12, 1982, to November 16, 1982. These data were recorded on five analog tape cassettes recovered on May 26, 1983, (Byrne et al., in press). Processing to obtain spectral noise levels was accomplished by passing the analog signals through an H-P 3582-A Spectrum Analyzer and

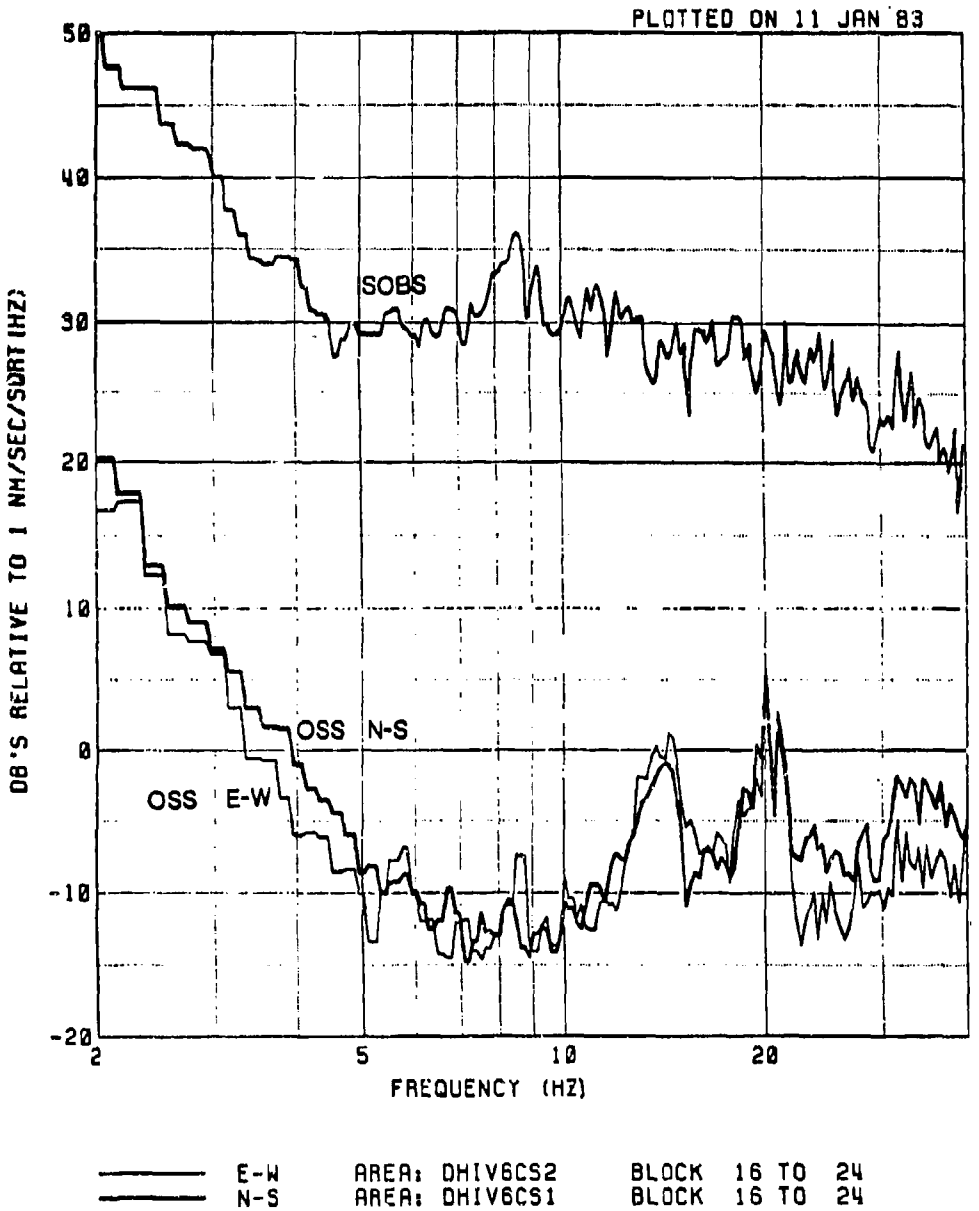

Figure 2. Same as Figure 1 for horizontal geophones.

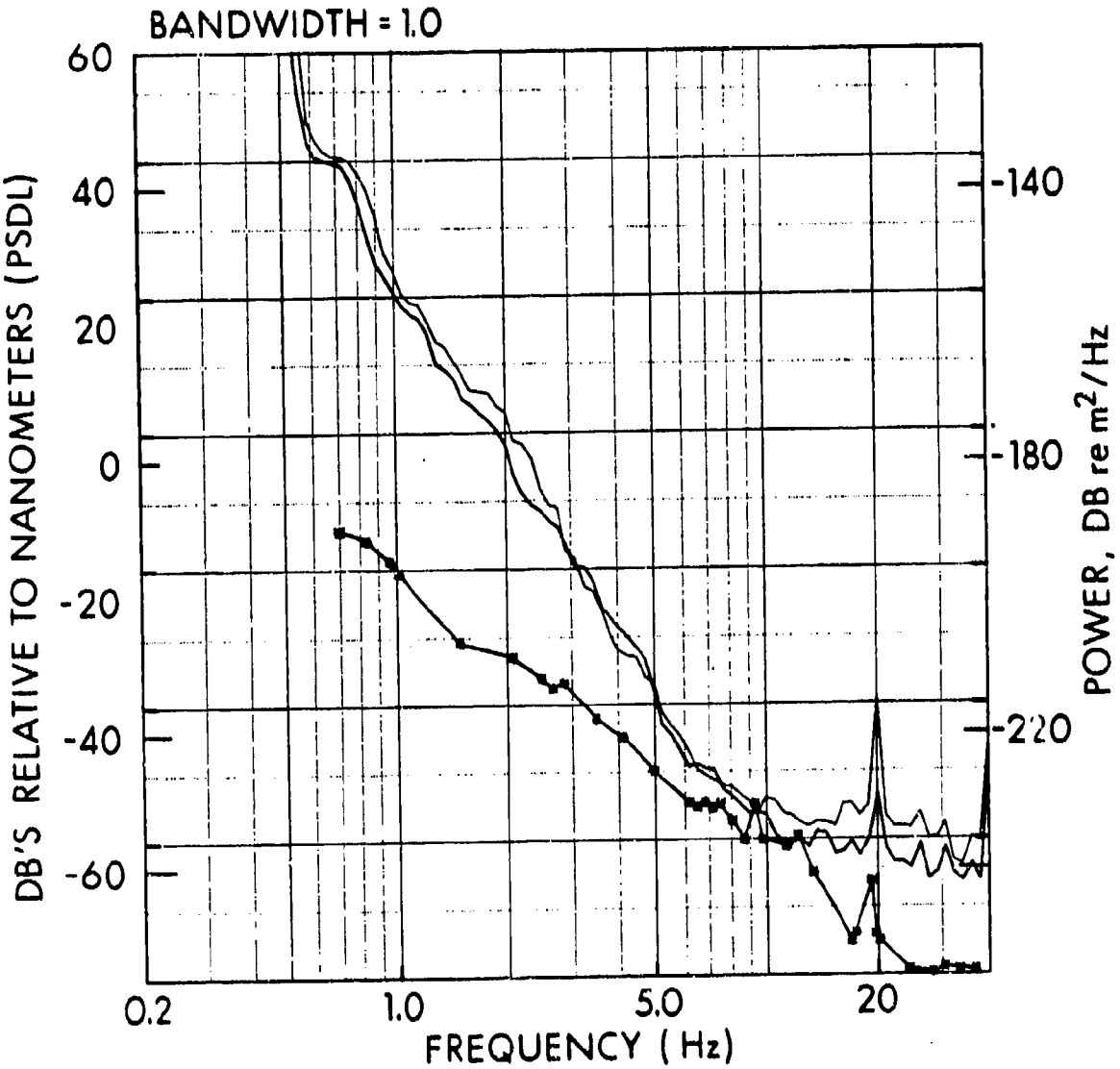

Figure 3. OSS noise levels at nine months after emplacement compared with a quiet continental seismic borehole station (Lajitas, Herrin, 1982).

capturing the digital output (2 spectra averaged every 28 minutes). See the Appendix for details of data reduction for Figure 4. These spectra were averaged and filtered to obtain signal levels in 6 frequency bands shown in Figure 4 for the two horizontal axes. Also plotted are the atmospheric pressure and pressure gradient measured from weather maps every 12 hours. There is a strong correlation between high atmospheric pressure gradients and high noise levels above 4 Hz. High pressure gradients indicate the passage of storms over the site, and thus indicate that noise levels can be increased by as much as 12 to 18 dB by storm wave activity at the ocean surface. The sensitivity of the instrument to acoustic "noise" is also demonstrated by the fact that the splash from a 6-lb. SUS charge dropped from a P-3 aircraft directly over the hole was well recorded by the vertical geophone.

Also of interest in Figure 4 are the variations in low frequency noise. Near day 280, for instance, a drop of almost 12 dB occurs at frequencies below 6 Hz, lasting for about 5 hours at 5 Hz, 8 hours at 3 Hz, and more than 10 hours below 2 Hz. Drops in noise level of this type occur several times in the record at times when atmospheric pressure is high and pressure gradient is low, thus possibly correlating with very quiet sea conditions.

The peaks lasting for several hours on the record are noise caused by the passage of ships near the site. More than 120 signatures of ships were recorded during the 64-day period, and signals from at least one ship are nearly always visible on the record. A sample spectrogram of data is shown in Figure 5 with frequency on the vertical axis, time horizontal, and amplitude levels shown by the darkness. Two ship "lines" are visible, one at about 8.25 Hz with multiples at 12.5 and 16.5 Hz, and a second broader

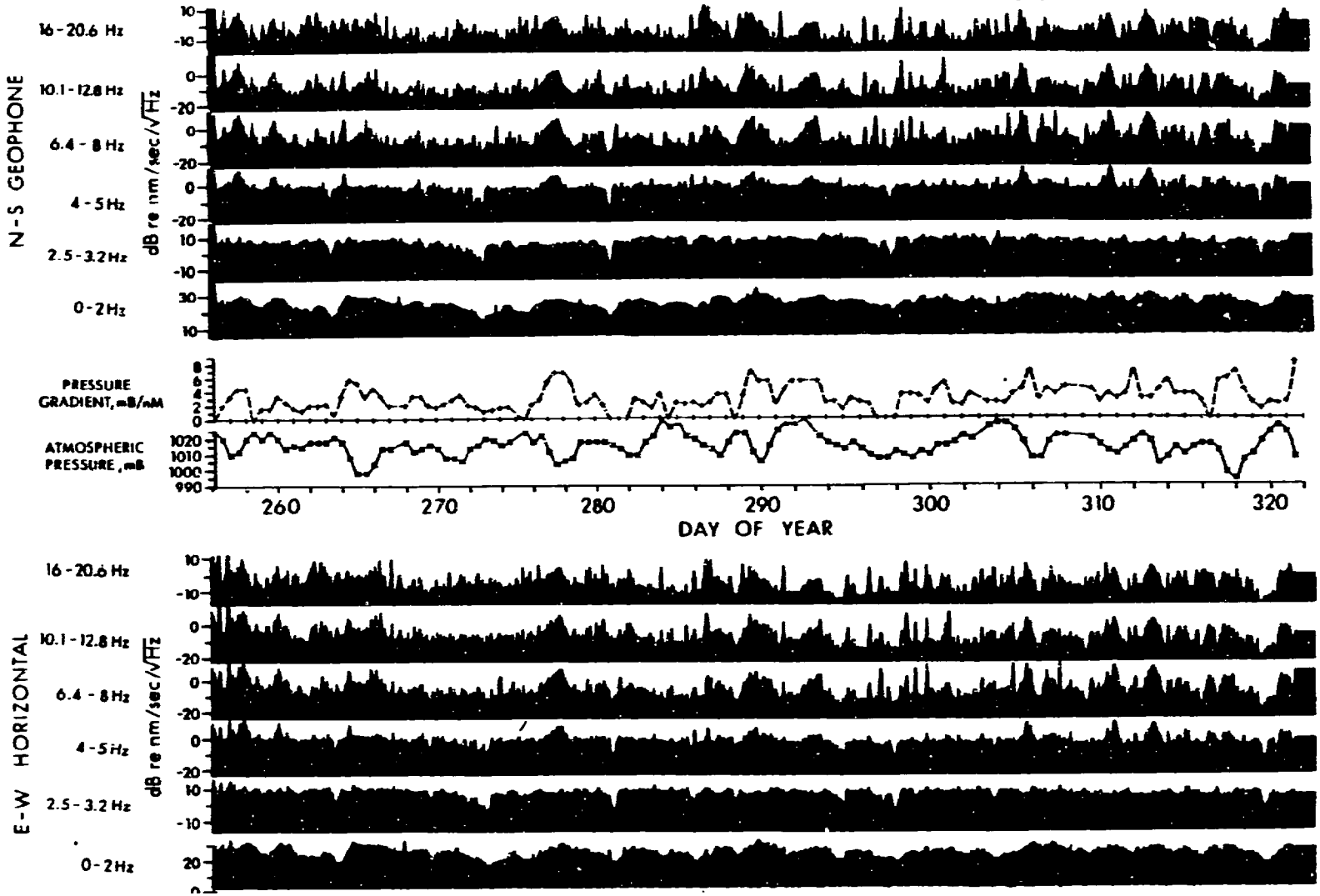

Figure 4. Seismic background noise level versus time for the OSSIV site. The noise levels versus time for the two horizontal geophones are shown in various frequency bands and compared with atmospheric pressure and pressure gradient fluctuations over the 64-day recording period. See the text and Appendix for discussion.

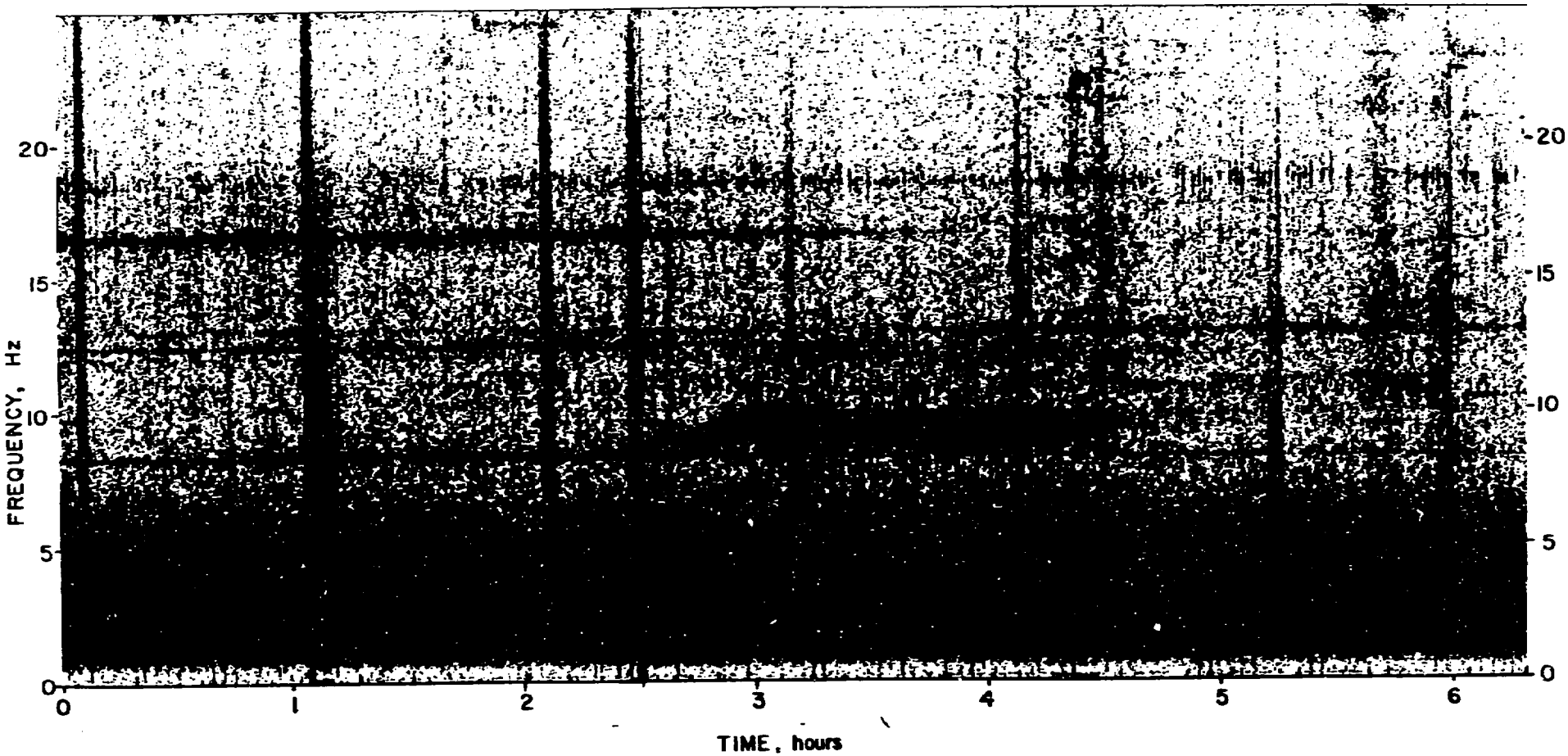

Figure 5. Spectrogram of OSS E-W horizontal noise for a 6-hour period during the 64-day recording period. The horizontal axis is time, with frequency on the vertical axis. Dark areas show high signal levels. At least two ships are visible, one with three lines at 8.25, 12.5, and 16.5 Hz, and the other broader band at 9-9.5 Hz. The vertical lines show the arrivals from earthquakes, and the intermittent signals at 18.5 Hz are believed to be from a whale.

peak between 9-9.5 Hz. Several earthquakes are visible as vertical black lines in pairs (P and S).

The ships are of interest in that there is enough information in the signal envelopes to determine the ship course with a 4-way ambiguity, and ship speed and range if the source level is known. As shown in Figure 6, the signature of a passing ship is much different on each axis. The signal should reach a maximum on the vertical at closest approach, but the horizontals can have two peaks, and will have an amplitude minima when the ship is at an azimuth perpendicular to the sensitive axis. The smooth curve shows a theoretical fit to these data using a propagation loss function of

$$A = A_o r^{S}$$

where A_o is the source amplitude and S is obtained from propagation loss data discussed later. It is likely that studies of the phase correlation between components could resolve the azimuth ambiguity and provide range information.

Another common type of noise observed in Figure 5 is the pulses at 18 Hz. These pulses are about 8 seconds in duration with a higher frequency (near 22 Hz) normally directly followed by the lower frequency pulse. The pulses repeat about once every 65 seconds for 10 to 13 minutes and then skip a pulse before starting again. Rectified traces of this type of noise are shown in Figure 7. Similar signals were recorded by Northrop et al., 1970, on Midway hydrophones. They speculate that the source is a "large biological source" based on its slow speed and meandering path through the hydrophone array.

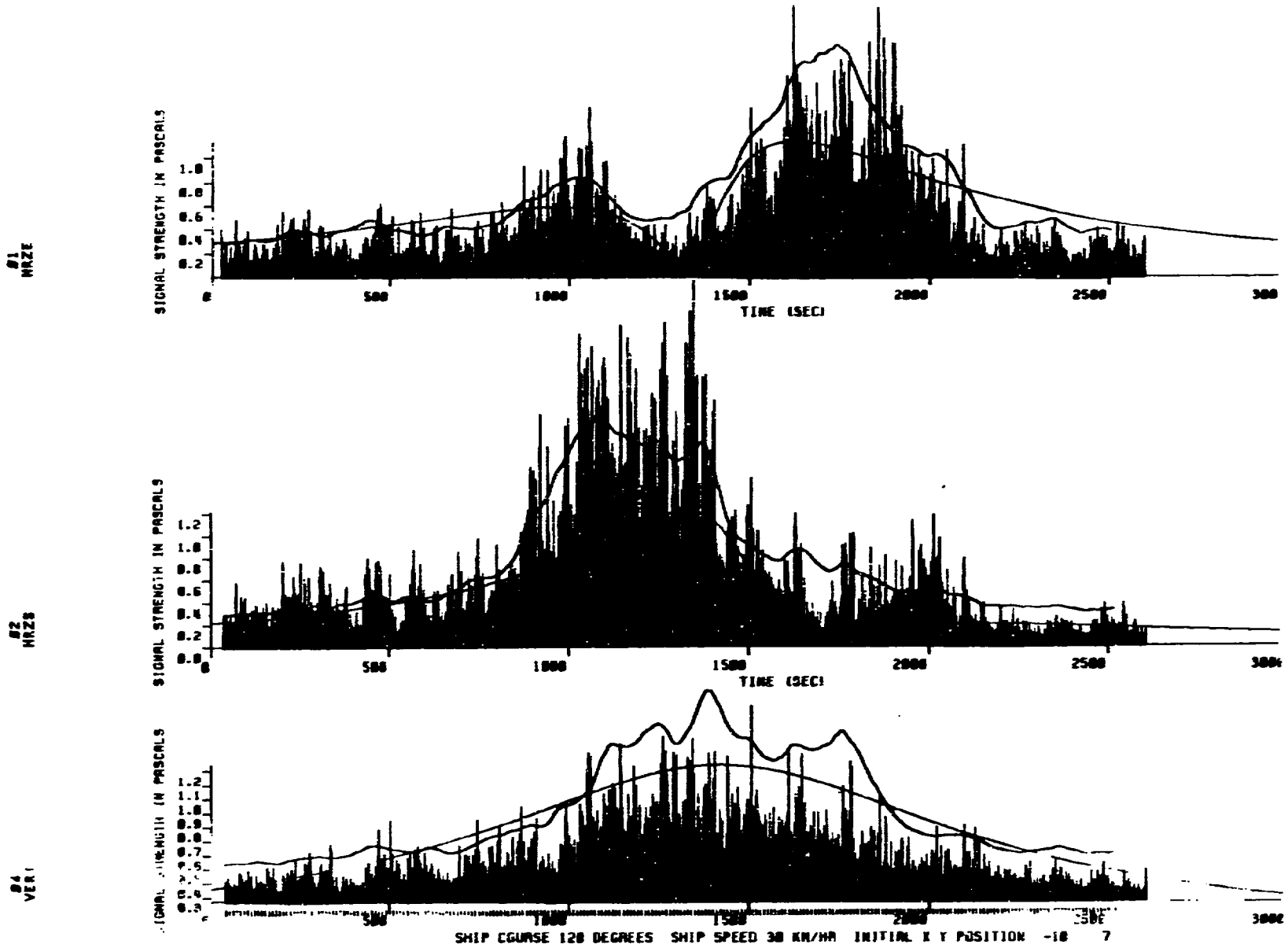

Figure 6. Signal from a ship recorded during the 64-day recording period. The rectified traces show the signal at 20 Hz and a broader band smoothed envelope function of the signal. The smoothed curve shows the theoretical amplitude function for a ship on a course of 120°.

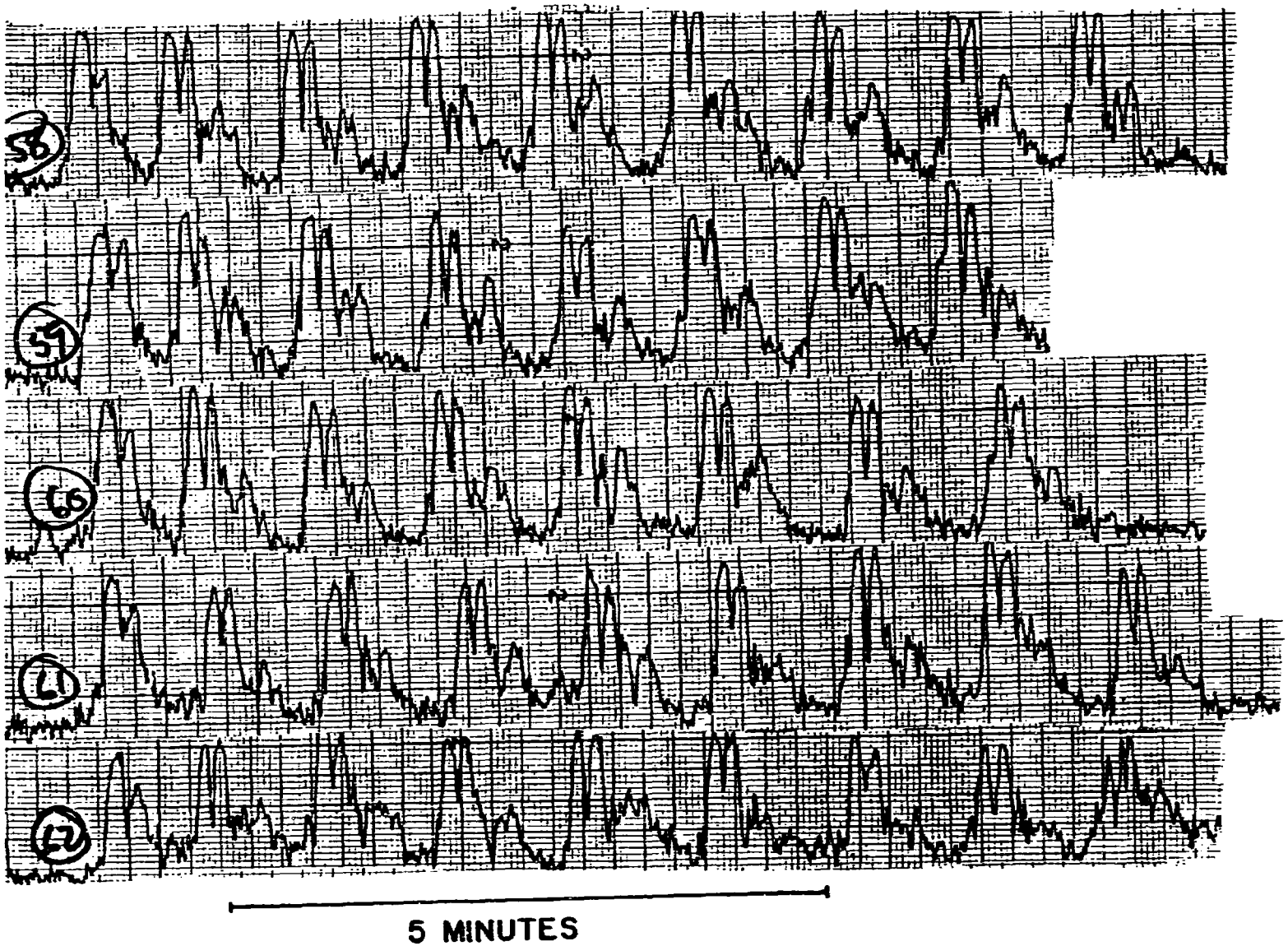

Figure 7. Rectified unfiltered signals believed to be from a large biological source recorded on a horizontal OSSIV geophone. The vertical scale is 5 dB per large division. Each trace follows the one above. The first peak in each pair has a frequency of about 22 Hz and the second about 19 Hz.

In some studies, earthquakes also become a source of noise. Regional and teleseismic earthquakes with S/N greater than 6 dB were recorded by the OSSIV geophones at a rate of about one per hour over the 64-day recording period (Cessaro et al., in prep). These events span the frequency range from 1 Hz and lower to about 20 Hz and last about three minutes on average; thus about 5% of the data contain earthquake signals.

When background noise caused by ships, storms, and earthquakes is low, the noise is dominated by instrument-generated noise caused by low-level aliasing of the digital transmission signal. This noise is present when voltages are about 5 μvolts and below at the input to the a/d converter (Byrne et al., in press). Testing of the system at these levels was not possible because of noise from other sources. It is important to note, however, that true seismic noise is lower than shown by the data at frequencies higher than 5 Hz.

III. Signal to Noise Comparisons and Propagation Loss. Unfortunately, very little data were collected on ocean bottom seismometers at the same time as OSSIV because the OSSIV emplacement was delayed until the last few days of Leg 88 by the aborted attempt to emplace the Marine Seismic Experiment. One short line of shots was recorded simultaneously on Oregon State University OBS #3 and on OSSIV. The time domain recordings of Shot #503 (16 pounds), 7 km from OBS #3 and 11 km from OSSIV are shown in Figure 8. First arrivals are well recorded at both stations, but the signals on OBS #3 are clipped early in the record (starting with the onset of the water wave arrival). Note that both the background and the signal on the OBS #3 horizontal component are resonant, with one dominant frequency. Spectra for these recordings are shown in Figure 9 for the first 2 seconds of signal before

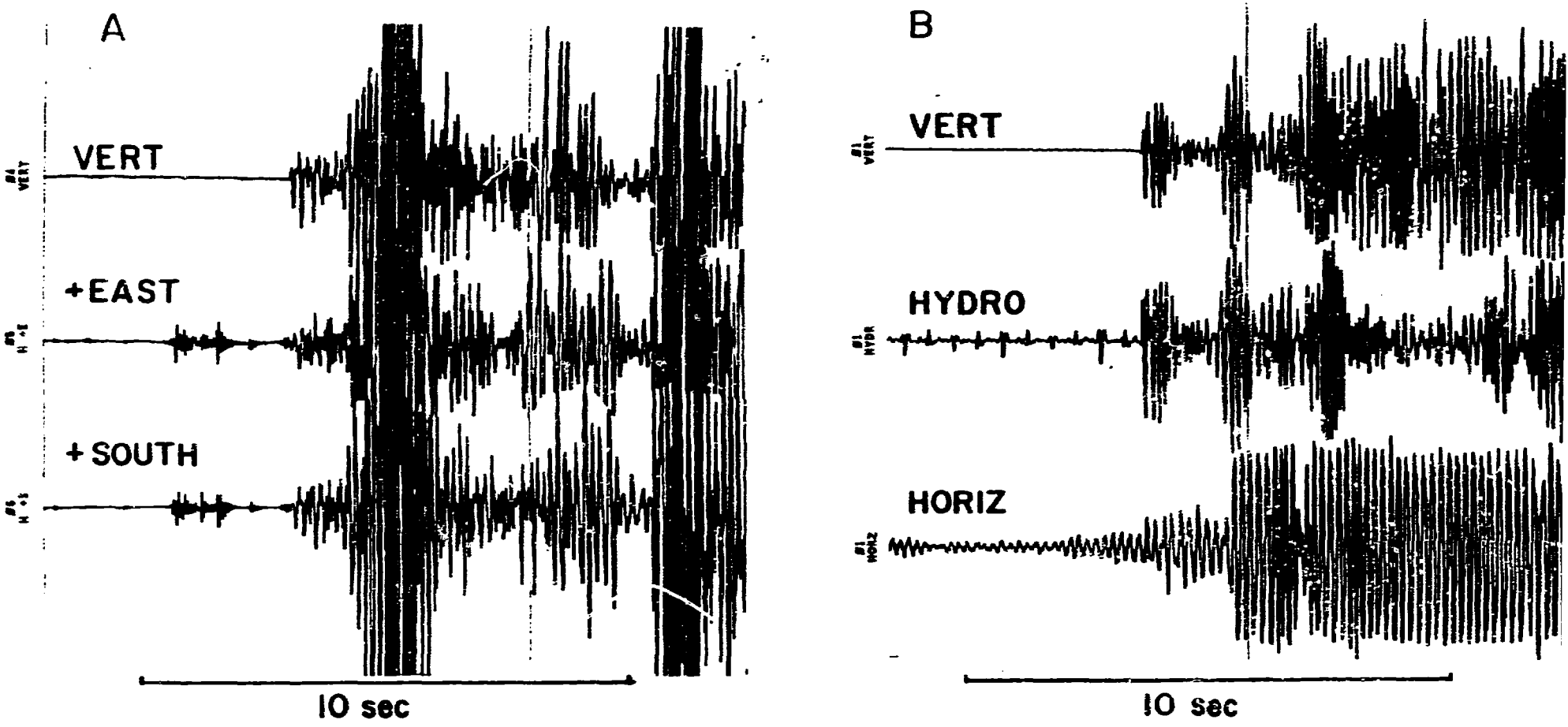

Figure 8. Time series from Shot #503. This 16-lb. explosion was fired by the USNS DE STEIGUER at a horizontal range of 7 km from the OBS and 11 km from OSSIV. Absolute amplitudes have not been calculated for these traces. They are shown to demonstrate signal quality. Figure 8A: Signals from OSSIV geophones. The noise in front of the horizontals is caused by material falling down the drill hole. Figure 8B: Oregon State University ocean bottom seismometer signals.

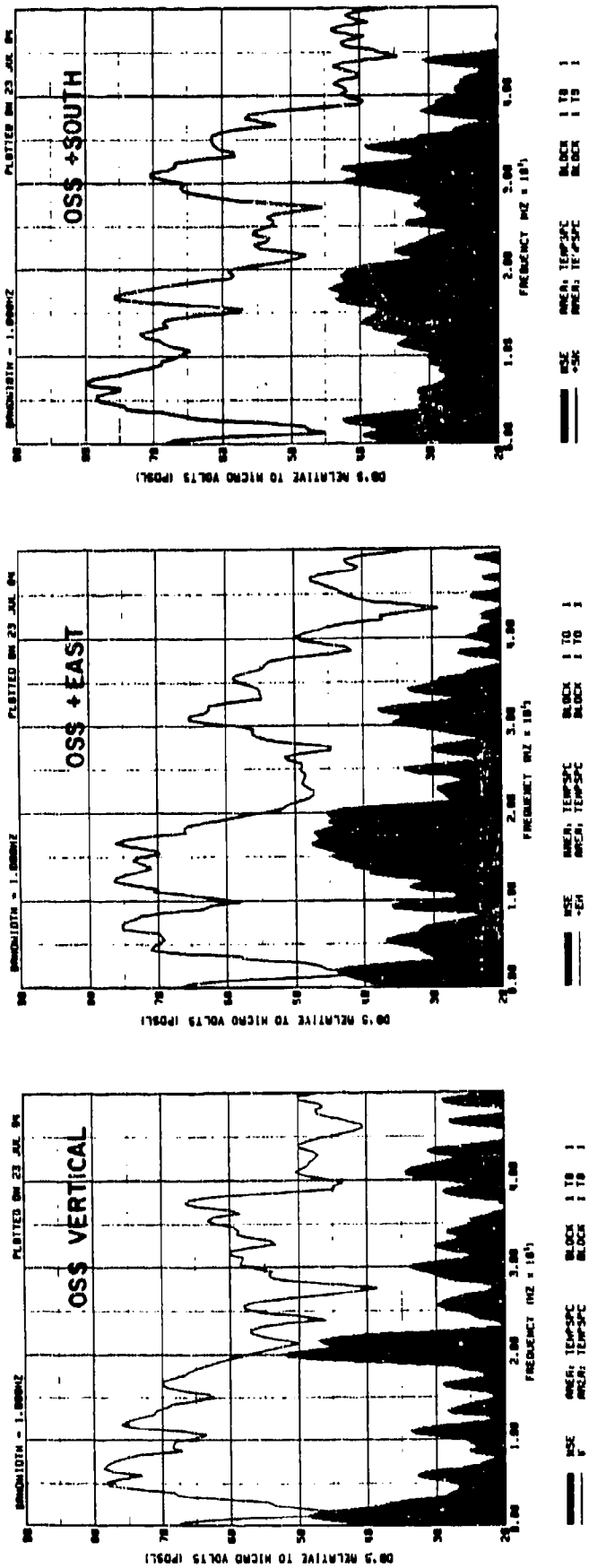

Figure 9A. OSS spectra from Shot #503. All spectra shown are for signals and noise prior to the onset of the water wave. All spectra are generated from 2.56 seconds of data (256 point FFT's). All signals are as recorded and are not corrected for instrument response.

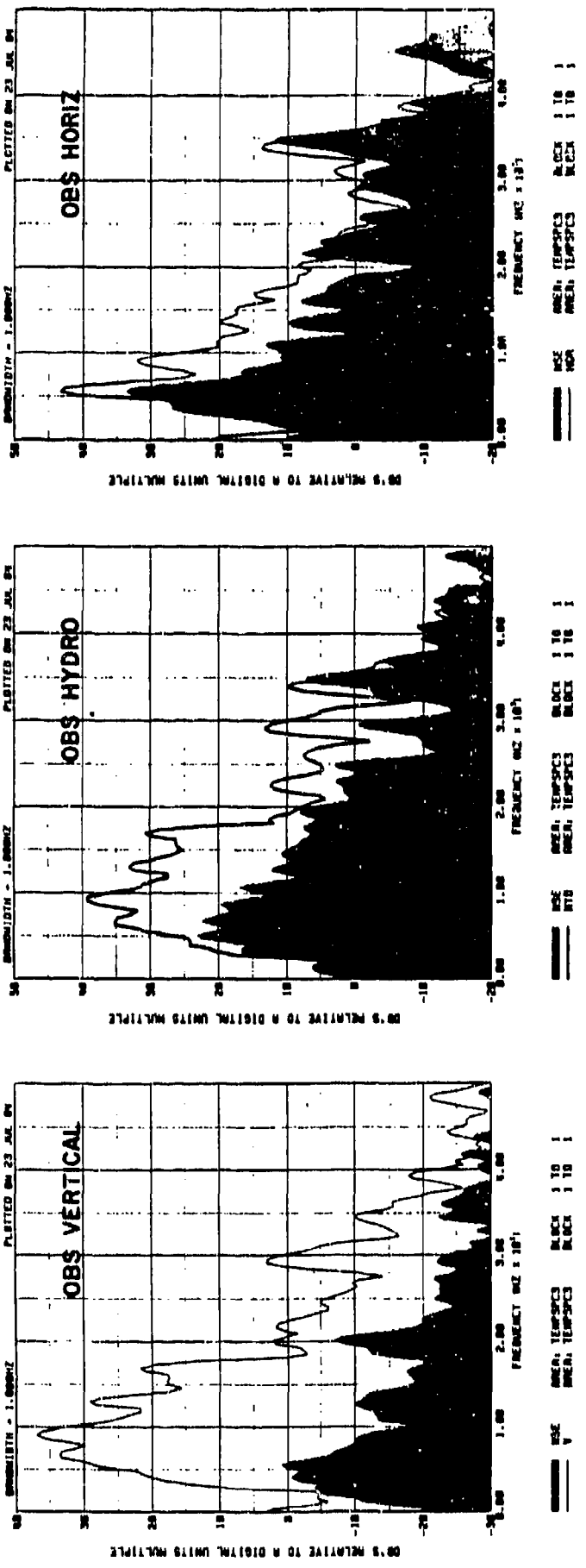

Figure 9B. OBS spectra from Shot #503.

the water wave arrival. Note that the OSSIV signals have a broader band signal than the OBS. S/N ratios are shown in Figure 10. The OBS vertical S/N is only slightly lower than the OSS between 7 and 15 Hz, but the OSS is far superior at lower and higher frequencies. The dip in S/N on the OSS near 20 Hz is caused by the large 20 Hz noise energy produced by the D/V GLOMAR CHALLENGER. Note also that the S/N on the OBS vertical component is about 18 dB better than on the hydrophone. This difference may be caused by system problems in the OBS. The resonance in the OBS horizontal component is most likely caused by poor coupling with the ocean floor; this is a common problem with OBS's, but one that can be fixed by proper design.

A second example of signals recorded on an OBS and the OSS is shown in Figure 11. These are recordings of two earthquakes, one made on an ISOBS (Byrne et al., 1983) and one on the OSS. The one recorded on the ISOBS had a magnitude of 5.0 and a range of 8.1° from the Kuriles, while the one recorded on the OSS had a magnitude of 4.9 and a range of 7.8°. Comparing the early arrivals (before the signals clip on the analog tapes), the S/N on the vertical components is similar between 4 and 10 Hz, but the OSS seems more sensitive at higher frequencies (Figure 12).

Unfortunately, there is no direct comparison of arrivals from acoustic signals with all or most of their travel path in the ocean. The OBS's that obtained successful recordings were all analog-recording, and the water wave signals are clipped. An instrument with the ability to record higher dynamic range (an OSU digital OBS) did not operate long enough to make the necessary recording.

An excellent data set was obtained to estimate propagation parameters of acoustic signals to the OSS during the reload of the instrument on May 26, 1984. A circle and two lines of explosives (practice depth charges, PDC

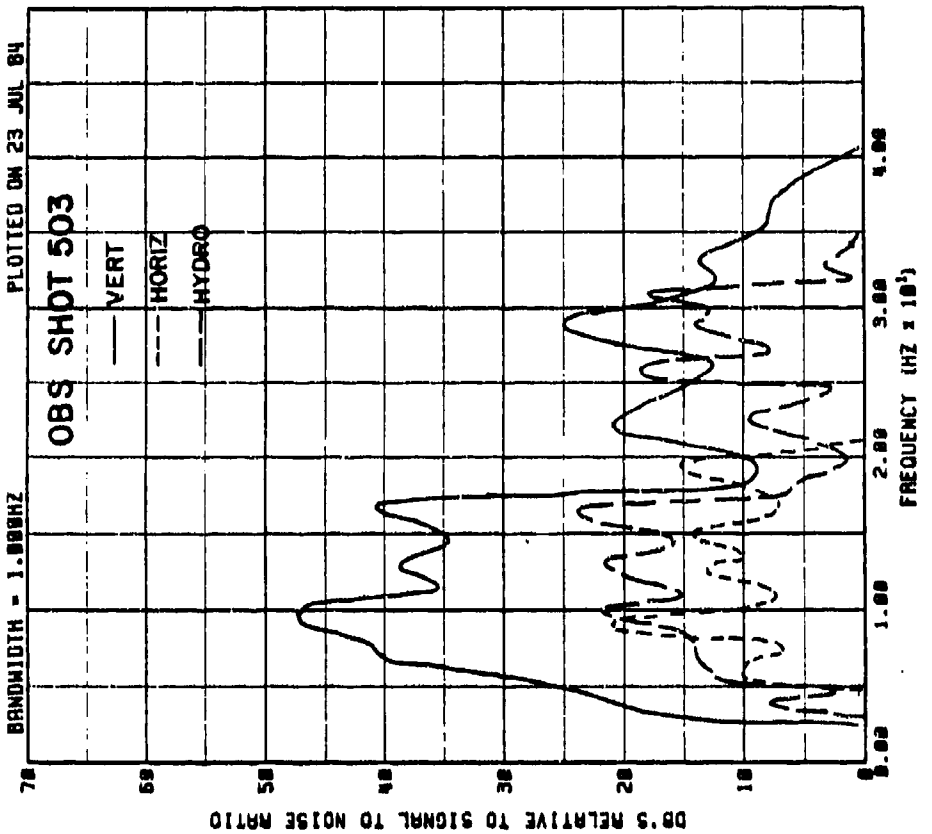

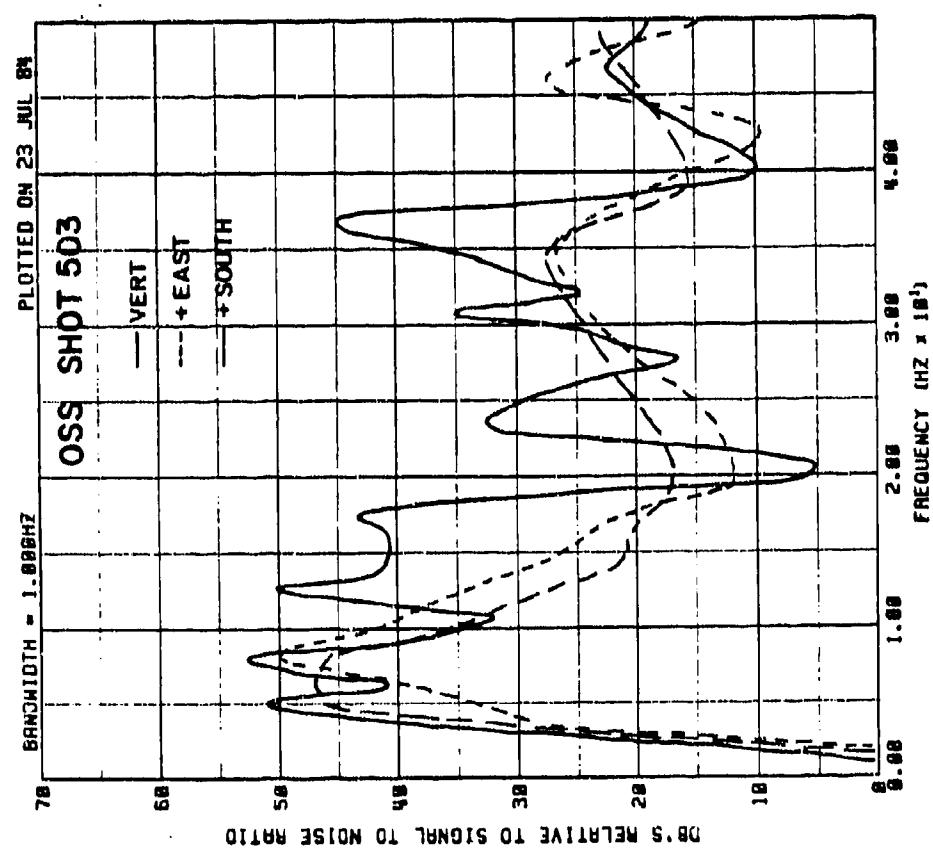

Figure 10. Signal to noise ratios from Figure 9. A. OSSIV geophones. B. OSU OBS.

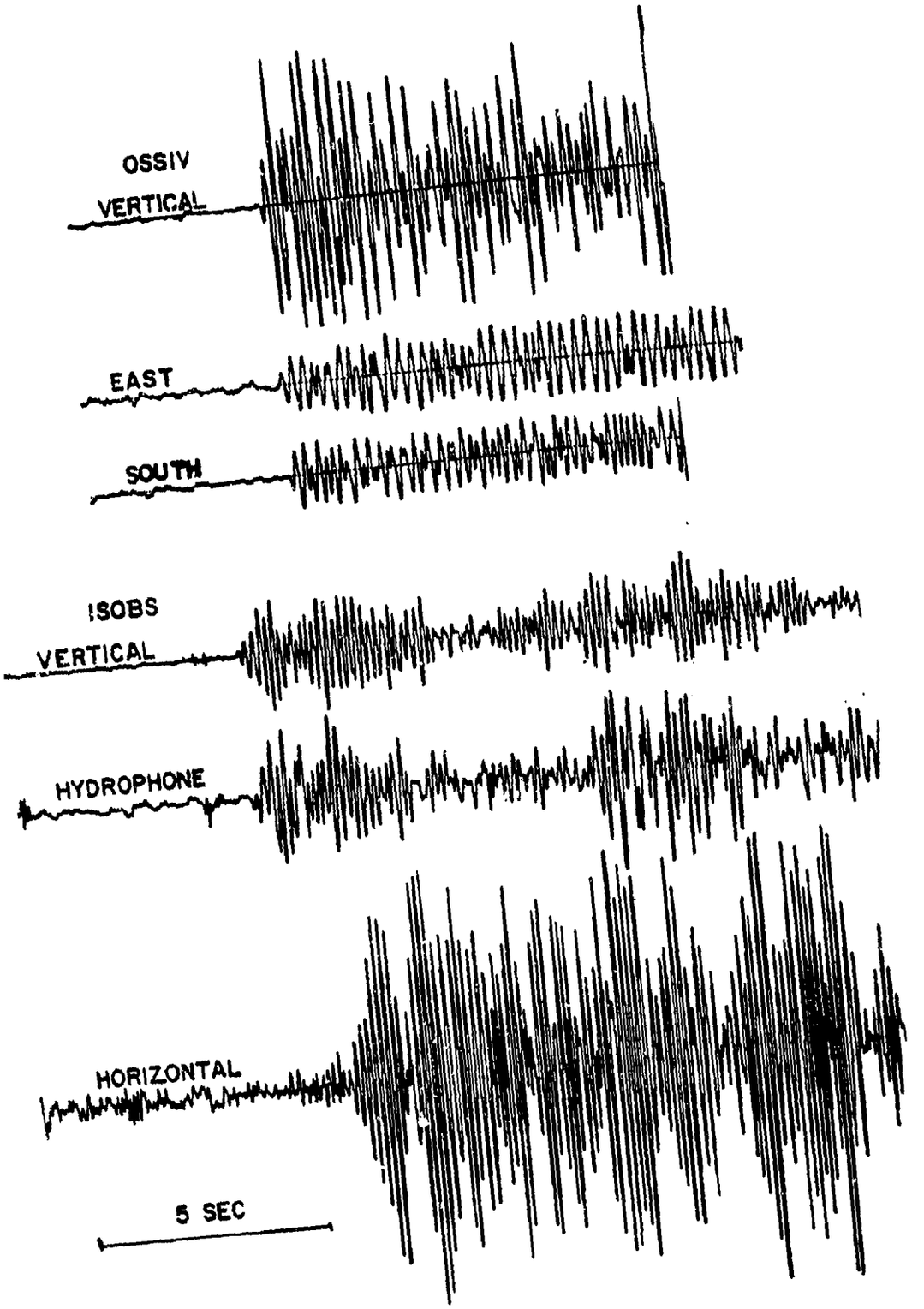

Figure 11. Signals from similar earthquakes recorded by OSSIV and an OBS. A. OSSIV recording of M_s = 4.9 earthquake from Kamchatka at a range of 7.8° (Oct. 30, 1982, 1625Z). B. ISOBS recording of a M_s = 4.9 earthquake from the Kuriles at a range of 8.3° (Sept. 6, 1982, 0037Z). Both events are normal depth (33 km). Severe clipping of the OSS horizontal geophones prevents comparison of S/N for these components.

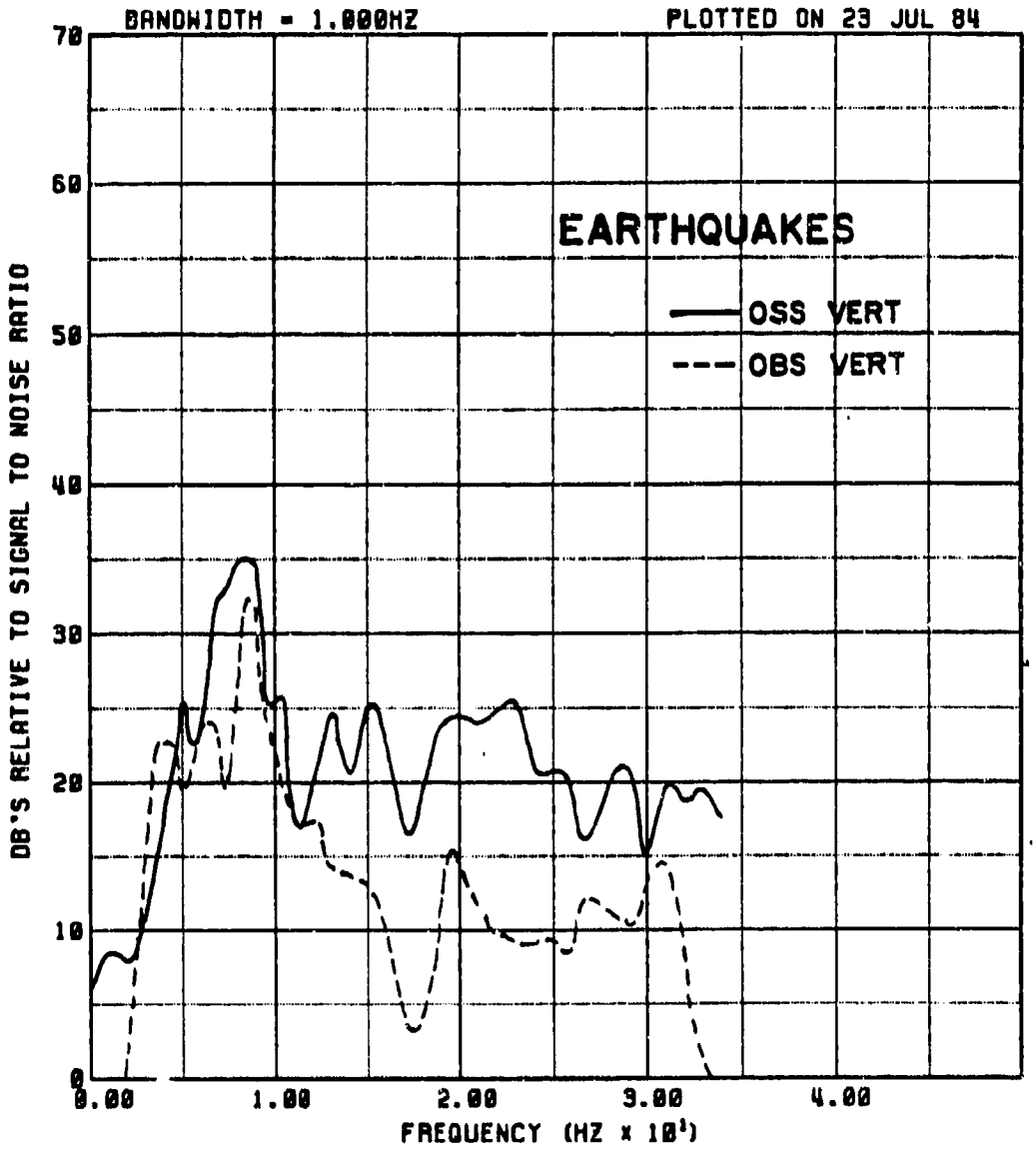

Figure 12. Signal to noise ratios for the vertical geophone first arrivals for the earthquakes shown in Figure 11.

Mark 64) were dropped by a Navy P-3 aircraft while the R/V KANA KEOKI was monitoring the OSSIV in real-time. Unfortunately, the circle was not recorded, but excellent data were obtained on a line from 0 to 90 km from the instrument. Each of the 29 (2-ounce) shots fired yields visible signals on the OSS, and the splash of the shot at zero range when the charge hit the water is also visible.

Analysis of these data is important to quantify the detectability of acoustic signals with sources in the ocean. The method used to obtain propagation loss (Figure 13) is explained in the Appendix. Also given in the Appendix are the transfer functions to change the output of the OSSIV geophones in μvolts to various units of ground motion, pressure, and propagation loss.

The propagation loss curves in Figure 13 show that loss at OSSIV is more than expected from spherical spreading, but the low noise level of the instrument makes it sensitive to sources in the ocean to long ranges. The shot line was from the east, thus less energy is expected on the N-S horizontal component than the E-W. This is the case over most of the line with the E-W component stronger by about 6 dB. Note that the zero-range shot is about 12 dB stronger on the vertical component than the horizontals. The propagation loss does not seem to vary with frequency in this band implying low attenuation.

It is of interest to determine where the energy is lost, since spreading does not account for the loss of signal. In an attempt to determine the amount of energy lost, we assume that a fraction of energy is transmitted into the earth each time the signal reflects from the ocean floor and the base of the sediments. The amount of energy lost is a

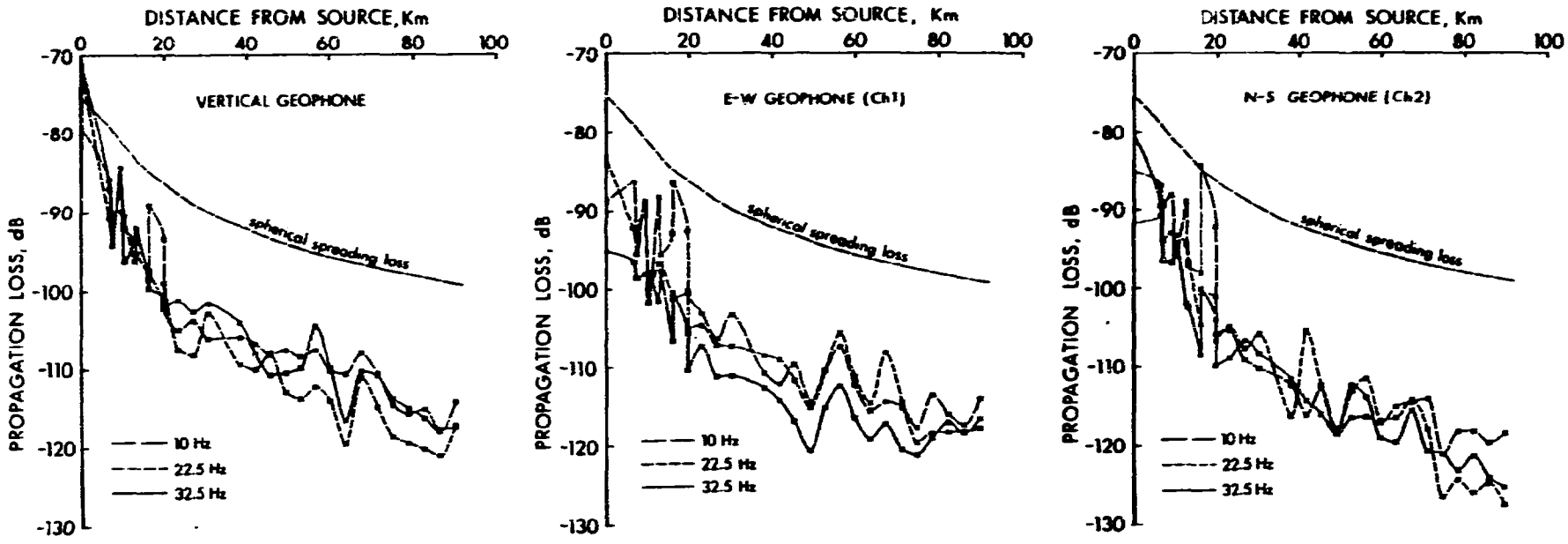

Figure 13. Propagation loss curves for OSSIV geophones obtained from SUS charge line (run approximately East-West). See text and appendix for explanation. A. vertical geophone. B. +East geophone. C. +South geophone.

function of the reflection angle. If the elastic properties of the water-sediment-crust system are known, then the partitioning of energy at each reflection can be determined (Aki and Richards, 1982). This has been done for the preliminary structure determined from seismic and acoustic records obtained at the OSSIV site (Figure 14). Individual water waves were then identified by their travel times, and their amplitudes were plotted (Figure 15) after spherical spreading correction, versus grazing angle (P). If a constant fraction of energy is lost per reflection for a particular angle, then the various reflections (direct, 1 reflection, 2 reflections, etc.) should be separated by equal amounts on a log amplitude scale. For most of the ranges encountered, most of the signal amplitude is shear energy and the energy lost per reflection from the ocean surface and basement is about 5 dB. These loss curves have been synthesized in Figure 16. The fit to the observations in Figure 15 is far from perfect, possibly because of scattering by bottom and surface roughness and imperfections in the model.

IV. Conclusions. Emplacement of seismic sensors in deep ocean drill holes can enhance detectability of earthquakes and acoustic events over what is possible using ocean bottom sensors. Waterborn acoustic signals generated in surface-limited ocean are almost certainly better detected by hydrophones in the sound channel. It is possible, however, that acoustic signals in shallow bottom-limited areas may be better detected by geophones buried in the ocean or in boreholes.

The removal of geophones from the ocean floor to hard rock in oceanic basement can greatly improve coupling and reduce signal complexity over that obtained from ocean bottom seismic sensors. It may be, however, that proper design of OBS's will largely negate this advantage.

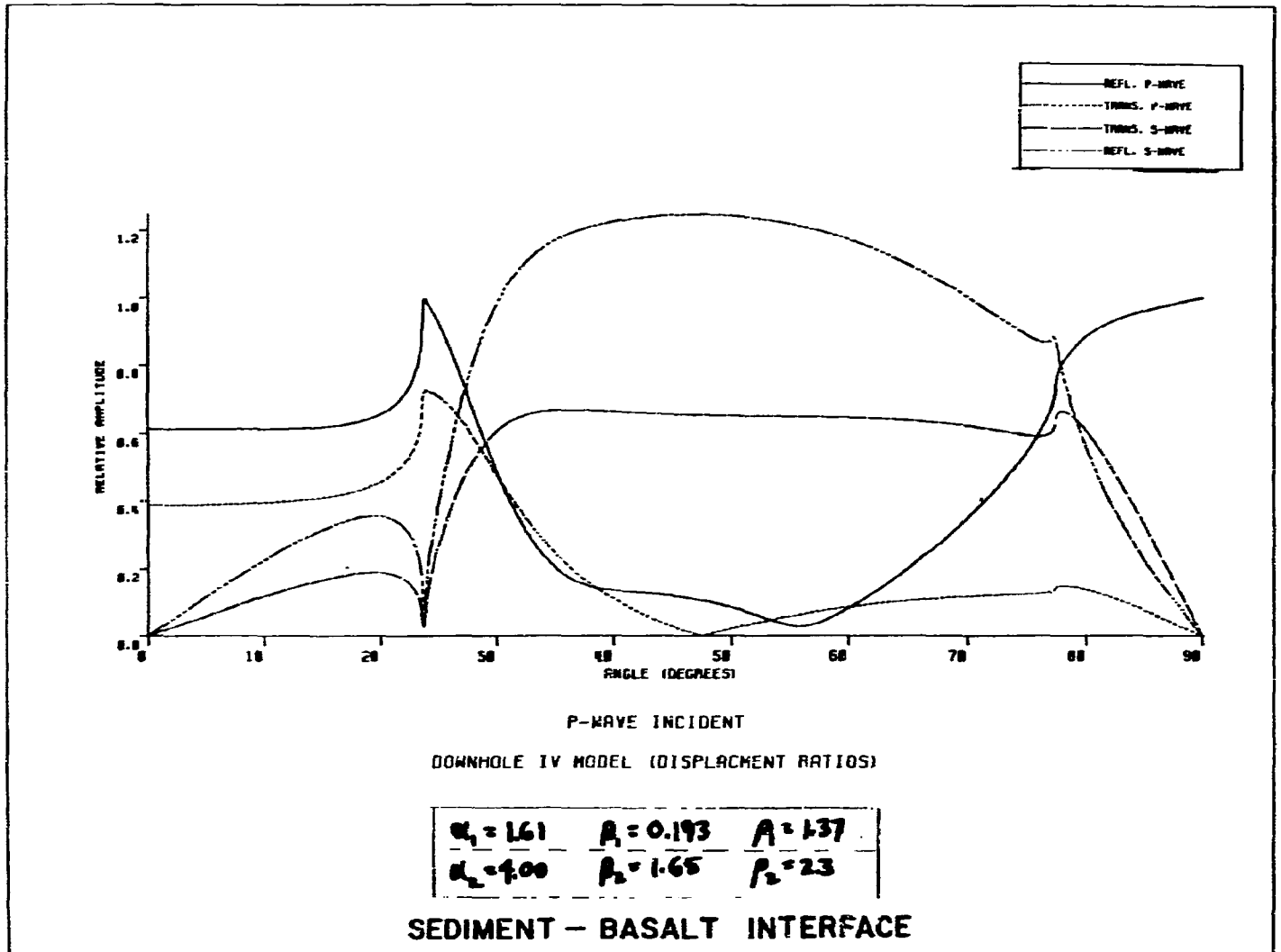

Figure 14. Amplitude reflection coefficients for the preliminary OSSIV elastic structure model of the sediment basalt interface.

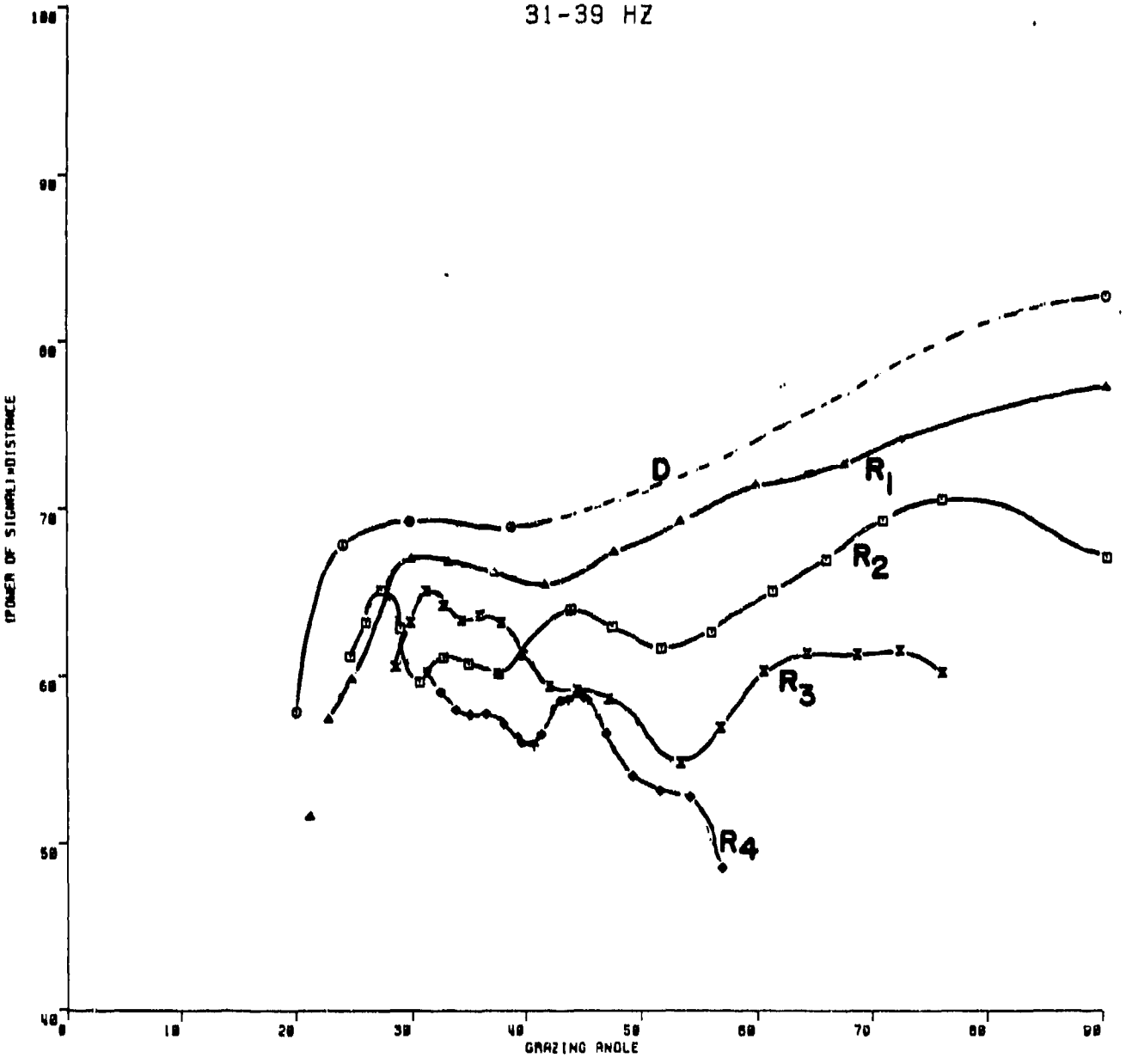

Figure 15. Water wave power versus grazing angle for the OSSIV SUS charge line. The values have been corrected for spherical spreading, thus the drop in power from one water wave to the next yields dB loss per bounce versus angle.

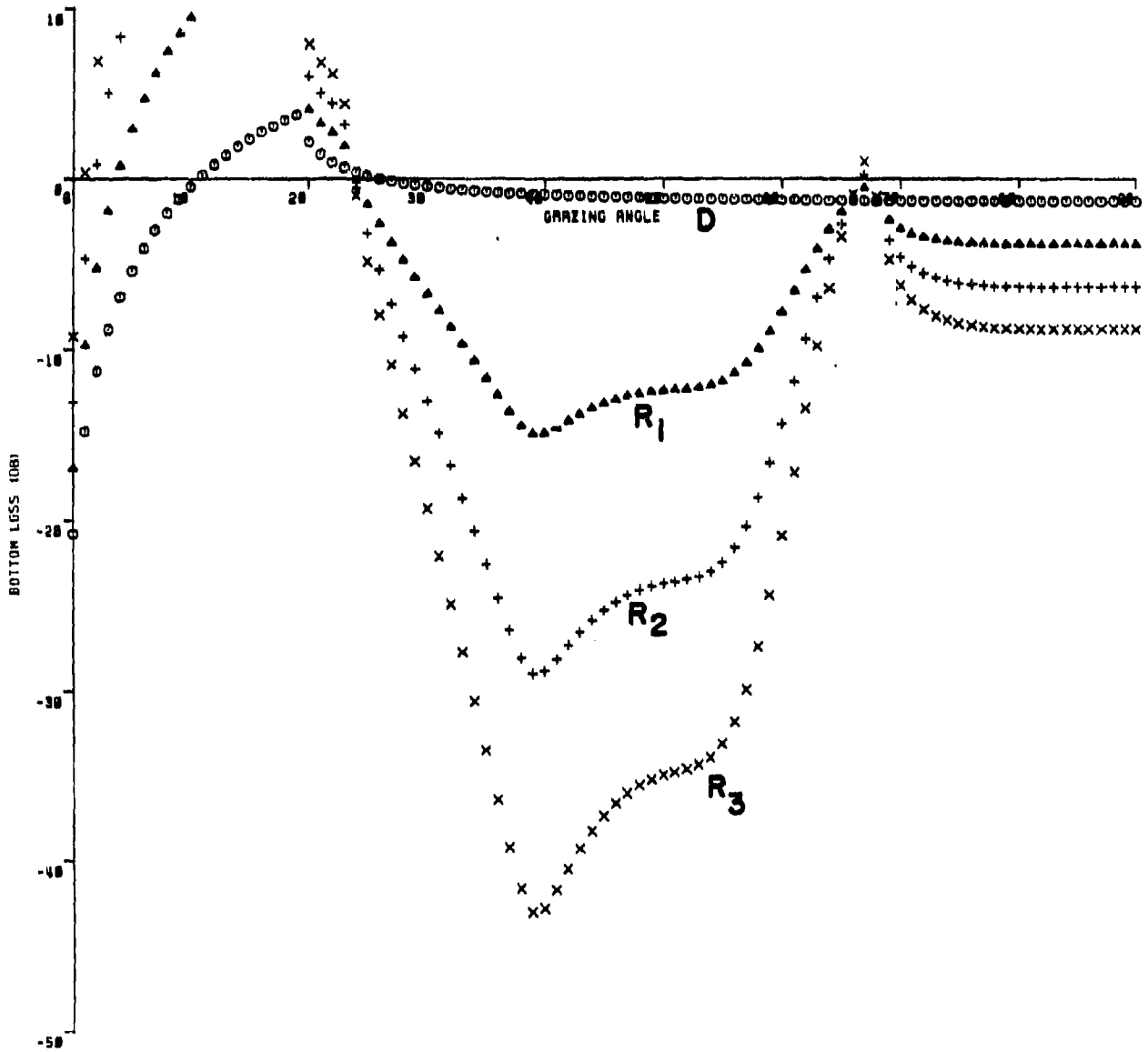

Figure 16. Theoretical version of Figure 15. The model reflection coefficients from Figure 14 predict greater propagation losses than are observed implying that the model needs improvement.

Open questions worthy of pursuing include:

1. Seismic signals: Is it profitable to emplace seismic systems in deep ocean boreholes to record earthquakes and explosions at very low frequencies (< 0.1 Hz) when compared to island stations and ocean bottom seismometers?

2. What are the effects of depth of burial? Must sensors be in basement rocks to achieve optimal results? How does detectability of acoustic signals change with depth of burial?

3. What are the effects of the water column? Will buried sensors detect acoustic signals better than hydrophones in the water in bottom-limited cases?

4. How will hydrophones respond in boreholes and when buried in the sediments?

5. What are the effects of variable bottom and sub-bottom structures on detectability?

Results from the OSSIV experiment, combined with those of the MSS 83 experiment, while not yet complete, will not be able to answer the above questions, and other experiments are needed.

APPENDIX

I. Computation of absolute noise levels from cassette recorded OSSIV data. Calculation of absolute noise levels from OSSIV seismic data recorded on the analog cassettes is relatively straight forward. Note that for the analog recorded data the nyquist frequency is 25 Hz (as opposed to 50 Hz for real-time data). Automatic gain control gains are allowed to change in 12 dB steps every minute on the minute if the noise level warrants a change. The gain level is recorded as part of the time code. (Ch 1 (E-W): sec 50-52, Ch 2 (N-S): sec 53-55, Ch 4 (vert): sec 56-58). Gain applied (B (g)) is shown below for each gain step:

g	B(g)
0	4 dB
1	16
2	28
3	40
4	52
5	64
6	76
7	88

The noise versus time data, shown in Figure 4, were processed through an H-P 3582-A Spectrum Analyzer directly from the cassettes. As the cassettes are recorded at 350 times slower than they are played back, frequencies on playback are 350 times those recorded, and one hour goes by in slightly over 10 seconds. The Spectrum Analyzer was set at the 10 kHz scale, uniform passband, two channel, averaging four spectra per output. At this scale each spectrum takes a time sample 12.8 msec in length (4.5 sec of OBS time). One output cycle required 4.8 sec, thus one spectral estimate (average of 4, 4.8 sec fft's) was made every 28 minutes of OBS time. As the band pass at these settings is 80 Hz (0.229 Hz, OBS frame), a 6.4 dB band

with correction was applied. These data were recorded on digital tape for later plotting.

Signal levels vary in the analog recording and playback process. The best way to determine this gain factor is as follows:

1. Measure the maximum p-p amplitude of the time code (Channel 3).

2. Multiply by 0.75 to obtain the equivalent unmodulated square wave amplitude.

3. Divide by 4.23 volts (the p-p equivalent square wave time code amplitude at the input to the cassette).

The resulting value is the net gain (or loss) in the record-playback process.

In many situations where it is desired to determine the absolute levels of spectral data, care must be taken to correct for bandwidth of the spectral estimates.

II. Computation of Propagation Loss. We know that the spectral level output by our FFT, $|X(j)|$, {defined by $X(j) = \frac{1}{N}\sum_{K=0}^{N-1} x(k)e^{-i2\pi jk/N}$ } is equal

to $\frac{\sqrt{2}}{2}$ times the RMS value of the time series (in digital units) in the band represented by the X(j).

ie., RMS(μvolts) = $\sqrt{2}\ |X(j)|$ (for 1 digital unit = 1 μvolt)

Now, to find the average particle velocity RMS u = $\bar{u}$, we must divide by the conversion factor, c(j), in $\frac{\mu\text{volts}}{\text{cm/sec}}$ taken from the calibration curve for the system.

{Note: c(j), like X(j), is a function of frequency where j has a one-to-one correspondence with some frequency.}

$$\bar{u} = \sqrt{2}\,|X(j)|\,\frac{1}{c(j)}$$

But what we want to find is the energy-flux-density, E_o, of our observed signal {E_o for E-observed} defined by:

$$E_o = \frac{1}{\rho_o c_o}\int_0^{\infty} p_o^2(t)\,dt$$

$$= \frac{1}{\rho_o c_o}\int_{t_o}^{t_1} p_o^2(t)\,dt$$

where the entire signal of interest lies between times t_o and t_1.

If we know the mean-squared value of $P_o(t)$ between t_o and t_1, $\overline{P_o^2}$, we can define E_o by:

$$E_o = \frac{1}{\rho_o c_o} \overline{p_o^2} (t_1 - t_o)$$

Assuming that pressure can be converted to particle velocity by the following expression, $P = \rho c u$, then

$$E_o = \rho_o c_o \overline{u^2} \Delta t \qquad (\text{for } \Delta t = t_1 - t_o)$$

Substituting for $\overline{u}$ gives:

$$E_o(j) = \rho_o c_o 2 |X(j)|^2 \frac{1}{C^2(j)} \Delta t$$

And taking the $\log_{10}$ of both sides and multiplying by 10 yields:

$$10 \log_{10} E_o(j) = 10 \log_{10} |X(j)|^2 - 10 \log_{10} C^2(j) + 10 \log_{10} (\rho_o c_o 2 \Delta t)$$

Now, if we define the propagation loss (actually the propagation gain): $P = E_o/E_s$ where E_s is the energy-flux-density at some place near to the source, then

$$\begin{aligned} 10 \log_{10} P(j) &= 10 \log_{10} E_o(j) - 10 \log_{10} E_s(j) \\ &= 10 \log_{10} |X(j)|^2 - 10 \log_{10} C^2(j) + 10 \log_{10} (\rho_o c_o 2 \Delta t) \\ &\quad - 10 \log_{10} E_s(j) \end{aligned}$$

Now let us take a look at those terms:

$10 \log_{10} x(j)^2$ is the dB power level out of our spectrum program re 1 digital unit, or 1 μvolt.

$10 \log_{10} c^2(j) = 20 \log_{10} c(j)$ is the dB response of the system re μvolts/(cm/sec).

$10 \log_{10} \{\rho_o c_o^2 t\} = 10 \log_{10} [(2.3\ g/cm^3)(3 \times 10^5\ cm/sec)(2)(20.48\ sec)]$

$10 \log_{10} E_s$ is the dB energy-flux-density of the source and must be calculated for each source used, or using the method of Weston, 1960.

Values for changing OSSIV geophone output in microvolts (1 digital unit = 1.0 μvolts) are given in the table together with conversions to other reference units.

particle velocity NANOMETER/SEC (PSDL)	displacement, velocity/(2*pi*f) NANOMETERS (PSDL) 12	PRESSURE AT OSS IN BASALT DYNES/CM**2 (RHO,C=2.3,3.0)	PROPAGATION LOSS TO OSS (MK64 AT 1 YD)
1. 05.7	1. 21.7	1. 28.9	1. 86.2
4. 29.7	4. 57.7	4. 52.9	4. 124.0
5. 32.7	5. 62.6	5. 55.9	5. 130.2
6. 33.7	6. 65.2	6. 56.9	6. 132.6
9. 33.2	9. 68.2	9. 56.4	9. 136.3
13. 31.5	13. 69.7	13. 54.7	13. 137.8
16. 29.9	16. 69.9	16. 53.1	16. 138.6
20. 27.9	20. 69.9	20. 51.1	20. 141.4
22. 27.0	22. 69.8	22. 50.2	22. 142.1
27. 25.3	27. 69.9	27. 48.5	27. 142.8
30. 24.3	30. 69.8	30. 47.5	30. 139.8
50. 20.0	50. 69.9	50. 43.2	50. 121.5

TRANSFER FUNCTIONS

The numbers in the table above are used to convert the output of the OSSIV geophones into useful units. The first number in each column pair is the frequency in Hz; the second number, when subtracted from a power spectral estimate (1 Hz bandwidth) at that frequency in dB re 1μvolt, yields dB referenced to the units given. Note that one digital unit of the OSSIV system is equal to 0.61μvolts.

REFERENCES

Adair, Richard G., J. Orcutt, and T. Jordan, Analysis of Ambient Seismic Noise Recorded by Downhole and Ocean Bottom Seismometers on Deep Sea Drilling Project Leg 78B. In Press, Let 78 Prelim. Science Report.

Aki, K. and P. Richards, Quantitative Seismology, Theory and Methods, Vol. 1, Sect. 5.2, W.H. Freeman, San Francisco, 1980.

Byrne, D., G. Sutton, G. Blackinton, and F. Duennebier, Isolated Sensor Ocean Bottom Seismometer, Marine Geophy. Res., Vol. 5, pp. 437-449, 1983.

Byrne, D., D. Harris, F. Duennebier, R. Cessaro, Technical Review of the Ocean Sub-Bottom Seismometer System Installed in Deep Sea Drilling Project Hole 581C, Leg 88, in press, DSDP Init. Reports Leg 88.

Carter, J., F. Duennebier, D. Hussong, A Comparison Between a Downhole Seismometer and a Seismometer on the Ocean Floor, Bull. Seis. Soc. Amer., Vol. 74, No. 2, pp. 763-772, Apr., 1984.

Cessaro, R. and F. Duennebier, Regional Earthquakes Recorded by OSSIV, in prep. for DSDP Init. Reports, Leg 88.

Herrin, E., The Resolution of Seismic Instruments Used in Treaty Verification Research, Bull. Seismo. Soc. Amer., Vol. 72B #6, S61-S68, 1982.

Nichols, R., Infrasonic Ambient Ocean Noise Measurements: Eleuthera, JASA, Vol. 69, No. 4, pp. 974-981, Apr., 1981.

Northrop, J., W. Cummings, and M. Morrison, Underwater 20 Hz Signals Recorded near Midway Island, JASA, Vol. 49 #6, Part 2, pp. 1909-1910, 1972.

Urick, Robert, Principles of Underwater Sound for Engineers, McGraw-Hill, Inc., 1981.

Weston, D., Underwater Explosions as Acoustic Sources, Pro. Phys. Soc. London, Vol. 76 (Part 2), p. 233, 1960.

HAWAII APPLIED RESEARCH INC.
Contract No. N00014-84-C-0464
Project No. NR 083-702/4-06-84 (420)

PROGRESS REPORT NO. 2

0001AB

For the Period 9/1/84 - 11/30/84

During this reporting period, the work effort has been primarily directed toward reducing and reproducing data for transmission to Rondout Associates and Dynamics Technology Corp. Four of the ten days of the data requested have been shipped. The remainder is in the reduction process.

At this time Task I (Evaluation of the Detection Capability) is nearing completion, Task II (Source Identification) is approximately fifty-five percent complete, and Task III (Evaluation of Shallow Water Experiment) is in th : preliminary planning phase.

Overall, the project is progressing as scheduled and no delays in data reduction and analyses are contemplated at this time.

HAWAII APPLIED RESEARCH, INCORPORATED

Project No. NR083-702/4-06-84(420)

Item No. 0001AC Progress Report
May 18, 1985

I. Tasks completed. All major tasks are now completed with the submission of this progress report. One area is still being studied, however; the evaluation of a shallow-water experiment. Seismic modelling studies have progressed slower than expected, and the evaluation is not yet complete.

II. Current progress:

Task I. Evaluation of the Detection Capability of the Borehole Seismic System. A study of the noise level vs. time for two of the ocean-bottom seismometers used during the OSS-IV experiment, one at the hole and one 40 km to the south, has been accomplished. Because of logistic problems, these OBS's were operating for an 11-day period before OSS-IV was installed, and data overlapped with OSS-IV for only a few hours. The OBS data studied are from HIG deployed-sensor instruments; i.e., the two geophones, a horizontal and vertical, are deployed in a small package about 1 meter from the main recording package to improve coupling and decrease noise.

A plot of noise levels vs. time for the horizontal OBS geophone (top) and a hydrophone (below) for each OBS is shown in Figure 1. Together with these noise level traces is shown the atmospheric pressure gradient (related to wind speed) for the same period. The high region in pressure gradient (and noise level) shows the passage of Hurricane Gordon over the site. The plots reveal information on the relative noise and signal-to-noise levels between the OBS's and OSS-IV.

Hurricane Gordon increased the atmospheric pressure gradient near the site to 9 mbars/N mile on day 250, causing an increase in S/N near 12 Hz of about 10 dB on the OBS horizontal geophone and hydrophone. A similar but smaller storm passed over the OSS on day 278, increasing the pressure gradient to 8 mbars/N mile. This storm increased the S/N on the OSS horizontal geophones by more than 15 dB near 12 Hz. It thus appears that the borehole sensors yield at least a factor of two increase in sensitivity to ocean surface signals.

Nearly all changes in noise level on the OBS records (Figure 1) correlate with known activities during the OSS-IV experiment (Figure 3). No biological signals were observed, such as are very common in the OSS-IV data, and few ships. The OSS-IV noise levels above 4 Hz show an almost continuous background of shipping. This observation again implies an increase in detection capability of the borehole sensors over the ocean-bottom sensors.

Task II. Source Identification. All data reduction and transmission required by this task are complete. In addition, we have completed a directivity study of the OSS-IV geophones, to determine their sensitivity azimuths relative to the world. This was accomplished by studying particle motion of first arrivals from 20 explosives fired at various azimuths and ranges. As a result of this study, the directions of the geophones were determined to ±1.5 degrees. The azimuth to impulsive sources can be determined to within ±6 degrees. While conducting this study, we found that in order to satisfy geometric requirements of the navigation and azimuthal data, hole 581C had to be moved 550 m to the west of the location of the ship while drilling.

Task III. Evaluation of the Desirability of a Shallow-Water Borehole Experiment. This will be a major subject of the final report.

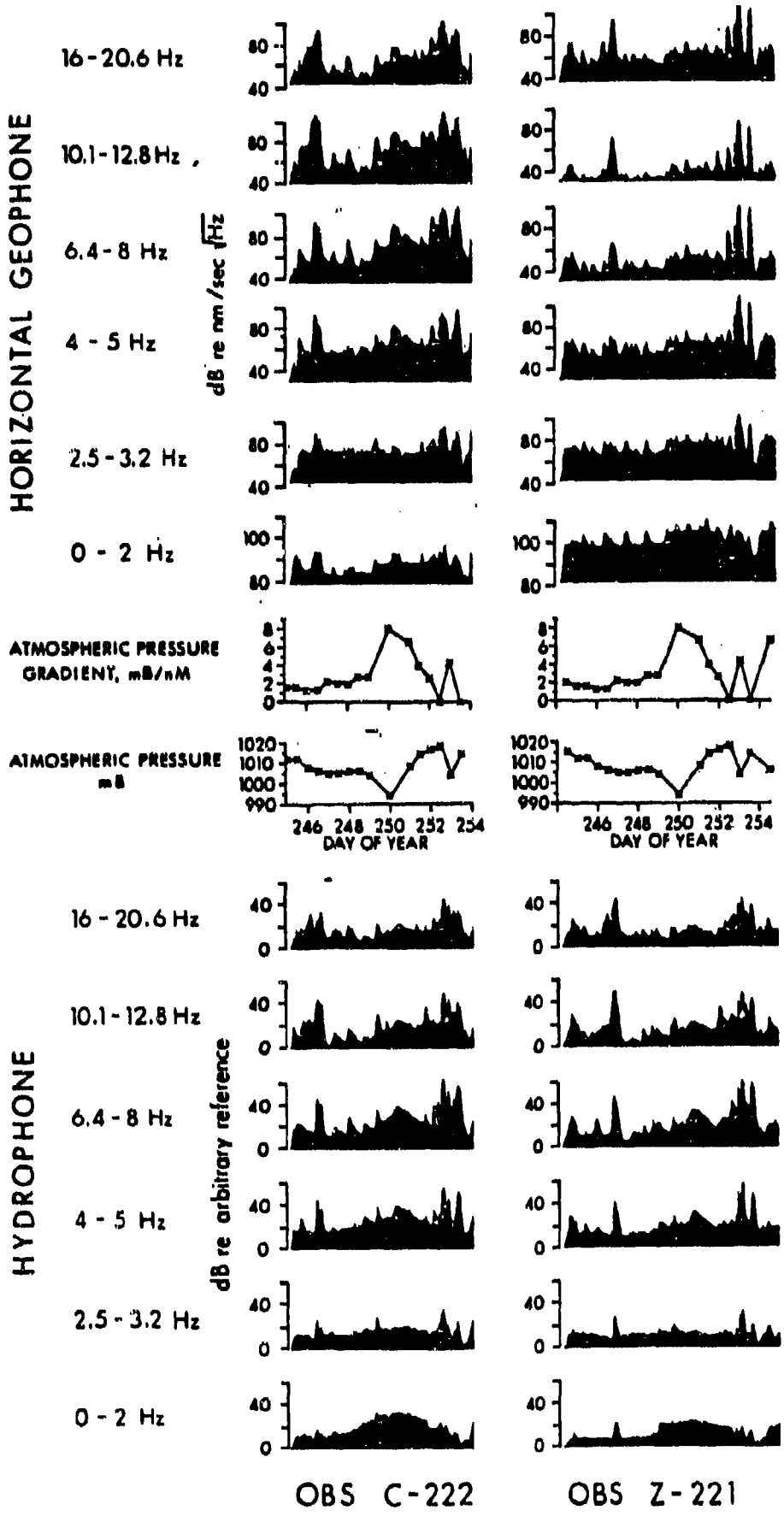

Figure 1. OBS noise levels vs. time during emplacement of OSS-IV. Also shown are the atmospheric pressure and pressure gradient for the same period. The large increase in level near day 250, 1982, is the passage of Hurricane Gordon.

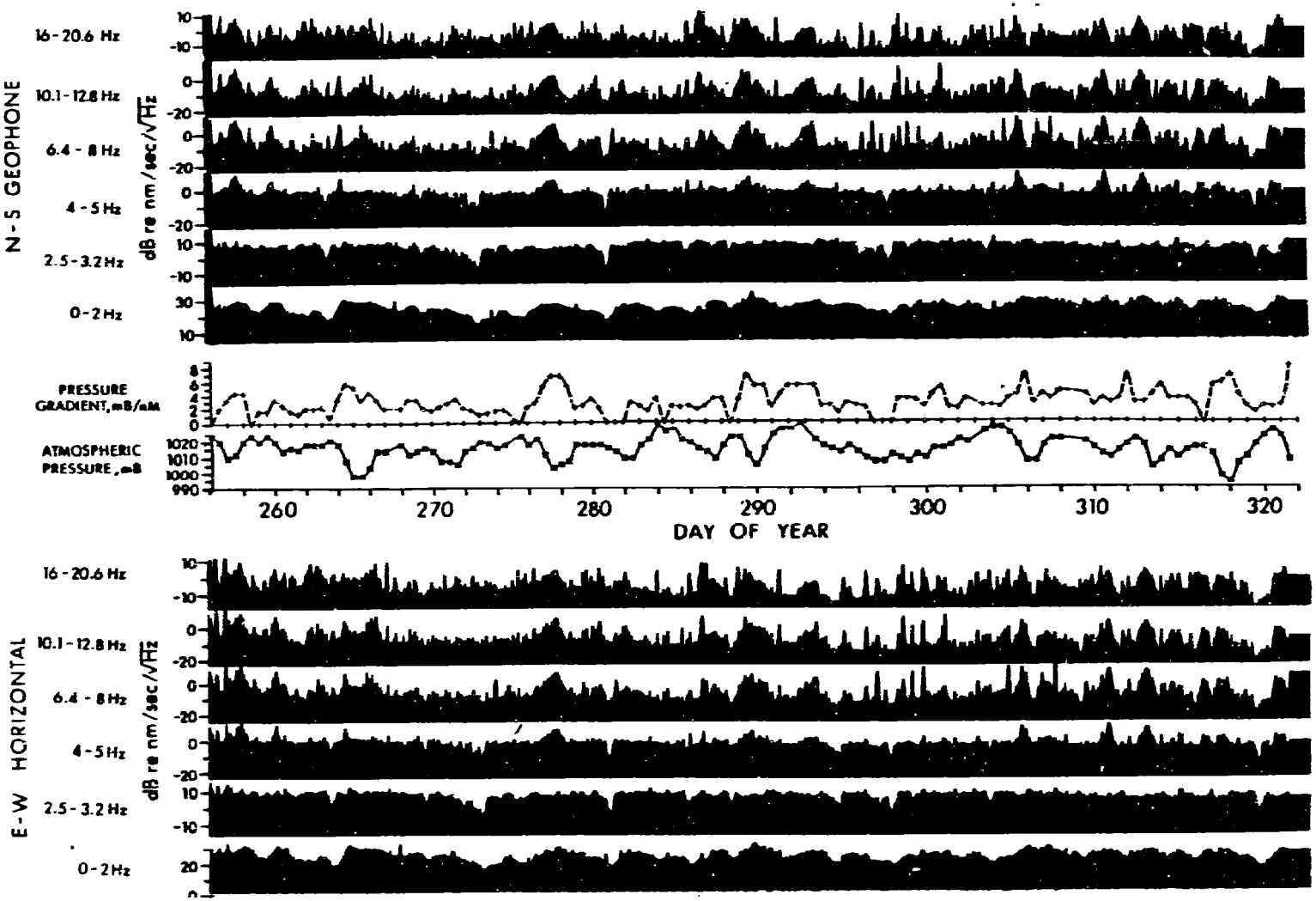

Figure 2. OSS-IV noise levels vs. time for a 64-day period in 1982. Also shown are the atmospheric pressure and presure gradient for the same time period.

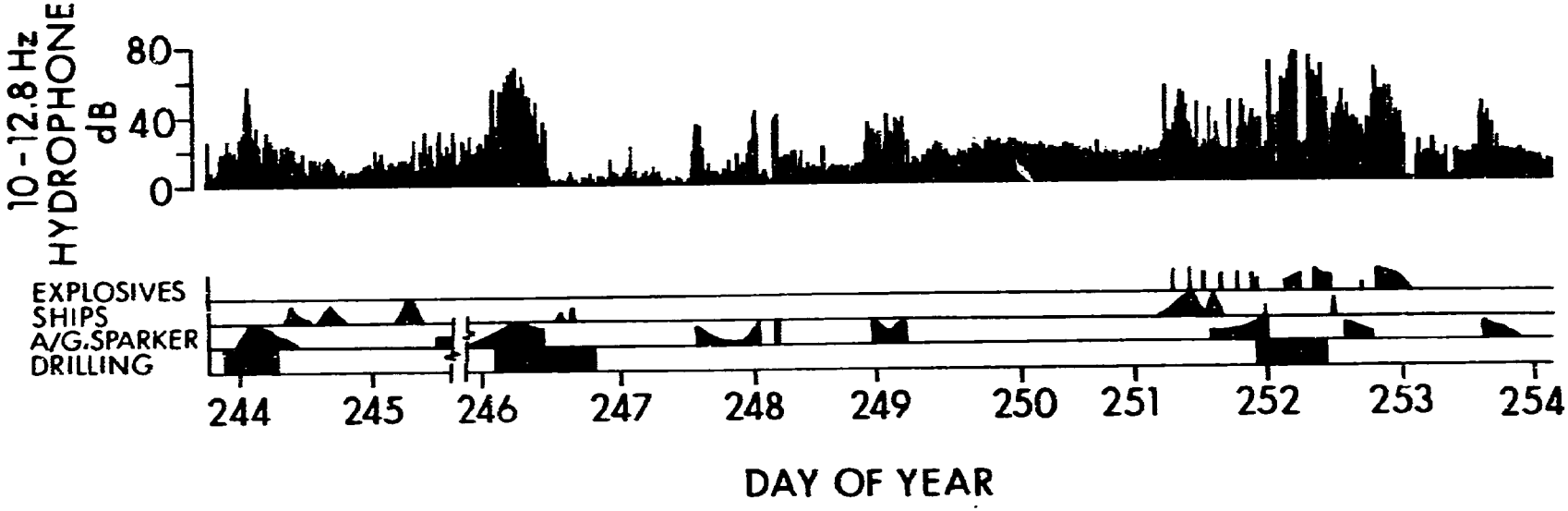

Figure 3. Correlation of OBS #221 hydrophone noise levels with activity near the drill site. The reference noise level for the hydrophone is unspecified.

TASK III

EVALUATION OF THE DESIRABILITY OF A SHALLOW WATER BOREHOLE EXPERIMENT

Acoustic Problem

Detection of acoustic targets in shallow water involves several problems not encountered in the SOFAR situation, all of which are caused by interactions with the ocean floor:

(1) low frequencies "leak out" of the ocean and are absorbed relatively quickly;

(2) direct paths from targets to receivers are extremely short, due to downward refraction of sound energy to the bottom, especially when the acoustic velocity in the water decreases beneath the source.

(3) Simple ray and acoustic assumptions break down because of varying (wedge-like) water depths and wavelength-dependent interaction with the ocean floor;

(4) the ocean floor is extremely variable because of local geological effects;

(5) ship traffic is often heavy, increasing noise levels:

and (6) the presence of Scholte waves complicates the sound field near the ocean floor.

Because of these problems, models for propagation that were adequate in deep water are inappropriate and inadequate for the shallow water case. Reasonably accurate modeling procedures (reflectivity codes, Stephens finite difference code, and the SAFARI codes) that allow lateral variations in depth and elastic properties are becoming available (Frazer and McCoy, 1985; Stephens, 1985), but their validity against real data has yet to be tested.

Some shallow water modeling studies indicate that a borehole receiver might be used to indirectly measure the acoustic wavefield in the water column. Preliminary models give general pictures of the propagation mechanisms in shallow water (Del Balzo et al., 1985; Doolittle et al., 1985; Frisk et al., 1985; etc.). These results predict that much of the energy propagating up slope is not lost, but is transmitted in and along the ocean floor. If this proves to be the case, then a borehole seismometer may well be a valuable tool for shallow water detection. Models also show that the energy maximum propagating down slope moves down with the bottom, indicating strong interaction with the seabed.

A borehole seismometer has a superior capability to couple with the seabed than the alternative instrument, the OBS, does. The quality of receiver-sea bottom coupling is a primary consideration in choosing an instrument to measure the wavefield present on the seabed. A borehole seismometer package, emplaced in solid rock or consolidated sediment, can be tightly wedged against the surrounding walls of the hole. The coupling of the receiver to the seabed achieved by this arrangement exceeds the coupling capabilities of an ocean bottom seismometer (OBS). A borehole seismometer can be expected to yield more accurate particle motion amplitudes (and, if three orthogonal geophones are used, particle directions also) than is possible with an OBS.

Putting the receiver in a borehole will prevent the recording of a portion of the field of rays including both signal and noise. Some of these rays will turn above the receiver. There will be attenuation while rays travel through overlying material, and some scattering of energy of subsurface inhomogeneities. The fraction of the total ray field reaching the receiver depends on the depth of the receiver in the borehole, as well

as on the properties of the overlying material. An optimum depth, which keeps the noise low level while still receiving the maximum portion of the signal wavefield, can be found.

While theoretical geoacoustic modeling at this point appears to be far from reliable, results indicate that shallow water low frequency energy may be best detected in boreholes. At shallow depths and low frequencies, the sediments are as much a part of the wave guide as the water. By installing geophones in boreholes, the excessive noise levels generated by low shear velocities in the shallow sediments, Scholte waves, and possibly much ocean wave-generated noise, can be avoided. Whether the possible increases in signal-to-noise and directivity can be realized can best be determined by careful experiment in areas of interest and under varied conditions.

Test Parameters

Given the question, "Can acoustic detection in shallow water be improved by emplacing sensors below the ocean floor?", several ancillary questions must be asked immediately:

(1) How deep below the ocean floor should sensors be placed?

(2) In what water depths can improvement be observed?

(3) At what source depths can improvement be observed?

(4) In what spectral regions are improvements observed?

(5) How does the improvement vary with:

  (a) sea state?

  (b) geological factors?

  (c) target direction relative to the bottom slope?

While it may not be possible to address all of these factors in a single test, it should be possible to consider most. At the very least, a

single three-axis geophone system should be emplaced with a hydrophone at the bottom of a shelf drill hole, together with a hydrophone and ocean bottom seismometer array. A calibrated wide-band source at a large variety of azimuths and ranges would then yield the necessary data. As time allows, the receiver should be moved upward in the hole a known distance and the experiment run again. With these data, and a reasonable choice of site, most of the questions asked above can be addressed.

Practical Considerations

Drill holes are very expensive to drill because of the high cost of drilling ships and crews ($50,000/day and up). Even a relatively shallow hole in an area requiring a minimum of transit time could easily cost $1,000,000 for drilling and emplacement. It may be possible to realize considerable savings by utilizing an existing borehole drilled either as a test well (such as the CAST wells in the Atlantic) or by the Deep Sea Drilling Project. If a drill rig is required for reentry, at least the drilling costs are saved. It may be possible to reenter many holes with experiments without a drill ship, using the Fly-In reentry techniques under study by several groups. With this method, the experiment is lowered into the hole from a bare wire supended from a standard research vessel, possibly with the aid of a submersible. In any case, the most difficult and highest risk part of this experimont is the successful emplacement of the borehole system. It would be very reasonable to see the emplacement through to a successful conclusion prior to the actual experiment in a two phase schedule.

As it is highly desirable to obtain data from several levels in the borehole. it would be advantageous to emplace a vertical array of sensors in

the hole. While this can be done with available technology, no such vertical seismic array exists, and it would need to be developed. Hydrophone arrays suitable for borehole emplacement do exist, and could be deployed with a minimum of effort.

As fidelity, dynamic range, and long recording time are valuable in experiments such as this, digital recording is called for, either with data transmitted to land or to a nearby ship. Real-time recording will also allow the experiment to proceed based on data quality, rather than by a fixed schedule.

In conclusion, a shallow-water borehole experiment appears to be justified and practical within reasonable costs. We would estimate that such an experiment could be completed within two years, and analysis of data completed in three years.

References

DelBalzo, D. R., J. E. Matthews, J. V. Soileau, and C. Feuillade, Acoustic propagation of large-scale linear ocean slopes, Publ. Plenum Press, NATO Conference Series, 1985.

Doolittle, R., A. Tolstoy, and M. Buckingham, Experimental confirmation of horizontal refraction of CW sound propagation in a wedge-like ocean, Publ. Plenum Press, NATO Conference Series, 1985.

Frazer, L. N., and J. J. McCoy, An acoustic reflectivity method for laterally-varying layered mediums, Publ. Plenum Press, NATO Conference Series,
1985.

Frisk, G. V., J. F. Lynch, and J. A. Doutt, The determination of geoacoustic models in shallow water, Publ. Plenum Press, NATO Conference Series, 1985.

Stephen, R. A., Finite difference seismograms for laterally varying marine models. J. Geophys. Res., 1985.

GEO-ACOUSTIC NOISE LEVELS IN A DEEP OCEAN BOREHOLE

F. K. Duennebier, R. K. Cessaro, P. Anderson

Hawaii Institute of Geophysics, University of Hawaii

2525 Correa Road, Honolulu, Hawaii 96822, U.S.A.

ABSTRACT. Noise levels recorded by a deep-ocean (5.5 km) borehole seismograph were found to vary by up to 20 dB during a 64-day continuous reading period. Noise level above 5 Hz is controlled by storms, shipping, and biological sources. Noise below 5 Hz appears to be completely controlled by sea state, even though the sensors are almost 6 km below the ocean surface. At least two mechanisms are observed for transmission of energy at the sea-surface to the ocean floor. One mechanism appears to yield seismic energy proportional to the wave energy apparently at a frequency twice that of the wave frequency (microseisms). This mechanism is observed at frequencies below 5 Hz. At higher frequencies, white noise is observed and increases in level with sea state. This energy is probably caused by breaking waves. Comparison of noise levels observed in the borehole with levels obtained by ocean bottom sensors at and near the site shows that weaker acoustic sources can be detected in the borehole than on the ocean floor, implying that low noise levels in the borehole more than compensate for signal loss.

INTRODUCTION

During Leg 88 of the Deep Sea Drilling Project, a permanent borehole seismic system was emplaced in hole 581-C (43.924°N, 159.797°E) by scientists from the Hawaii Institute of Geophysics. The instrument, Ocean Sub-bottom Seismometer IV (OSS IV), is clamped in place 20 m below the sediment-basalt interface, and 378 m below the ocean floor in 5.5 km of water. After a short check-out and seismic refraction experiment, an analog recording package was left at the site to record for the next 64 days. On May 25, 1983, the R/V KANA KEOKI returned to the site, recovered the recorded data, took data in real-time for about 24 hours, and then set out another recording package (which has yet to be recovered) (Figure 1). In addition to the OSS IV, eight Ocean Bottom Seismometers were emplaced at the site by the R/V DE STEIGUER. Unfortunately, there were only a few hours of overlap between the OSS IV and OBS data because of logistics problems. All together, more than 5000 impulsive acoustic sources and hundreds of earthquakes were recorded. In this paper, we ignore these signals of geophysical interest and concentrate on the noise spectrum and its temporal variations.

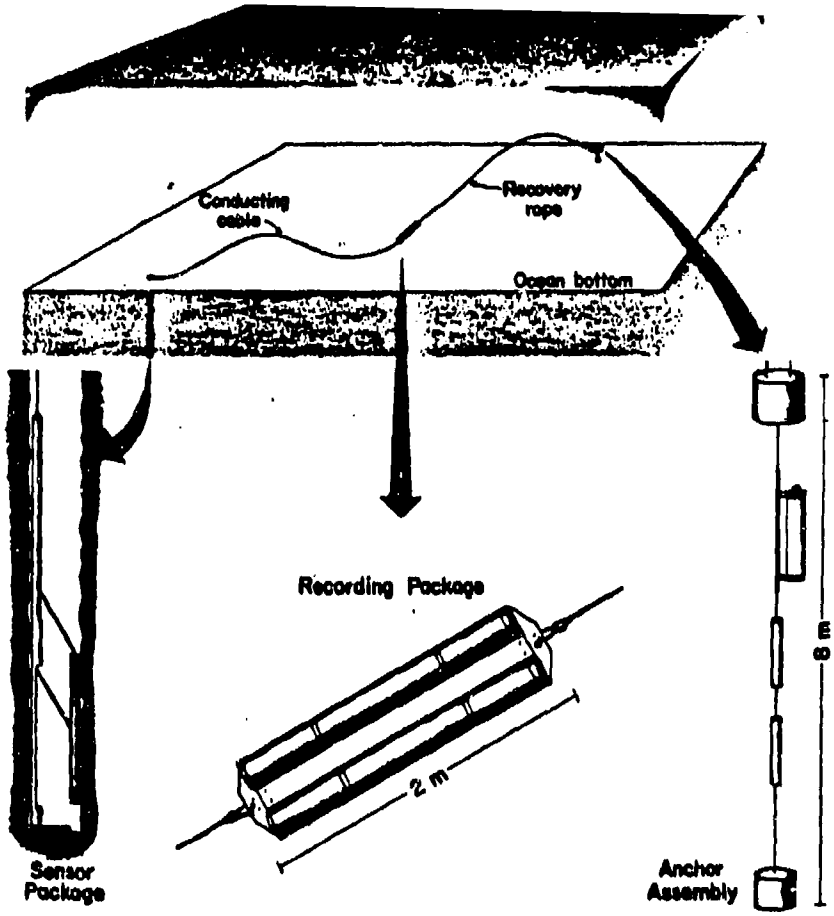

Fig. 1. Ocean Sub-bottom Seismometer. The sensor package, permanently locked at the bottom of the borehole, is powered by batteries in the recording package. The recording package is recovered by releasing the anchor from the anchor assembly.

INSTRUMENTATION

OSS IV contains three orthogonal 4.5-Hz geophone sensor groups that are capable of recording ambient background noise from about 0.2 Hz to above 20 Hz. The 20-Hz limit is determined by the 25-Hz Nyquist frequency, not the geophones. The vertical group contains nine geophones in series, and each horizontal group contains two geophones in series. Specific response curves and sensor characteristics are being published elsewhere[1]. The Hawaii Institute of Geophysics ocean bottom seismometers (OBSs) used in this study contain a vertical geophone, one horizontal geophone, and a hydrophone. The geophones are mechanically separated from the main OBS package to improve seismic coupling. Data quality from all sensors is excellent, although the calibration of the hydrophone is uncertain. Orientation of the horizontal geophones in OSS IV to within 1.5° has been accomplished by a study of the azimuths of arrivals from explosives at known locations[2].

The OSS IV geophone signals arrive at the recording package in digital form sampled at 50 samples per second per channel. The signals are converted back to analog in the recording package and recorded on three channels of a slow-speed analog cassette tape, with time code on the fourth channel. A C-120 tape can record up to 14 days of data, and fi[illegible]es were recorded sequentially with overlap. For this study sp[illegible] estimates were obtained directly from the analog tapes using a

Hewlett Packard 2318-A Spectrum Analyzer. Four spectra from each of two data channels were averaged about every 28 minutes of recorded time and stored in digital form for further processing. Thus, about 50 spectral estimates per day were used to generate the noise vs. time figures shown in this paper. Spectral levels have been corrected for gain changes (recorded with the time code) and the instrument response has been applied to the geophone traces.

DATA ANALYSIS

The complete noise history of the 64-day OSS IV data set is shown in Figure 2. Filter sections for five 1/3-octave bands and the energy below 2 Hz are shown for the two horizontal channels. The noise curves have been low-pass filtered to remove the numerous earthquakes that would otherwise stand out as "spikes" on the records. In addition to the seismic noise traces, two traces showing atmospheric information are displayed. These data were read from 12-hour satellite weather maps for the NE Pacific Ocean. The upper trace shows the atmospheric pressure gradient in millibars per nautical mile. This parameter should reflect wind speed. The lower trace shows absolute barometric pressure in millibars. High pressure generally corresponds to low wind speed and calm seas.

METEOROLOGICAL NOISE: Note that broad peaks in pressure gradient correlate with similar peaks in the noise level above 4 Hz and below 2 Hz. From 2 to 4 Hz the noise levels are nearly constant over the entire period, and there is little correlation of noise level with peaks in pressure gradient. The lack of variation in noise level between 2 and 5 Hz implies that the dominant noise generation mechanism at these frequencies is normally saturated. Only when the atmospheric pressure gradient is very low (implying no wind and calm seas) do the levels in this frequency band drop below the saturation level.

To further investigate the storm-related noise mechanisms, we have plotted noise level vs. frequency at six-hour intervals for the storm beginning on day 264 (Figure 3). Time period 1 was taken at the point of lowest noise level. Six hours later, noise level has increased to saturation between about 3 and 7 Hz, but has changed little below 2 Hz or above 7 Hz. Twelve hours into the storm noise level between 2 and 7 Hz is saturated and noise, levels to below 0.2 Hz have increased. Eighteen hours into the storm, levels to 1 Hz are saturated and an increase in noise level is observed above 5 Hz. Twenty-four hours into the storm the noise levels are at their highest. This behavior of seismic noise during a storm is similar to the energy spectrum of a developing sea during a storm. The ocean wave spectrum saturates at lower and lower frequencies as wind speed, duration, and fetch increase. The slope of the saturated portion of the energy spectrum is close to f^{-5}, the value expected for the saturated portion of the ocean wave spectrum[3]. The lowest noise level observed above 5 Hz is most likely instrument noise[4].

The mechanism by which the ocean wave energy is transmitted to and below the ocean floor is apparently the same as that which generates microseisms[5,6,7]. A non-attenuating pressure fluctuation field with frequency twice that of the ocean wave frequency is propagated downward. The Longuet-Higgins theory depends on the non-linear interaction of waves of the same frequency traveling in different directions, such as reflections from shore. Thus, the amplitude of the pressure wave produc[illegible] microseisms should be heavily dependent on shore configuration and s[illegible]haracteristics. The observation of the saturation slope from

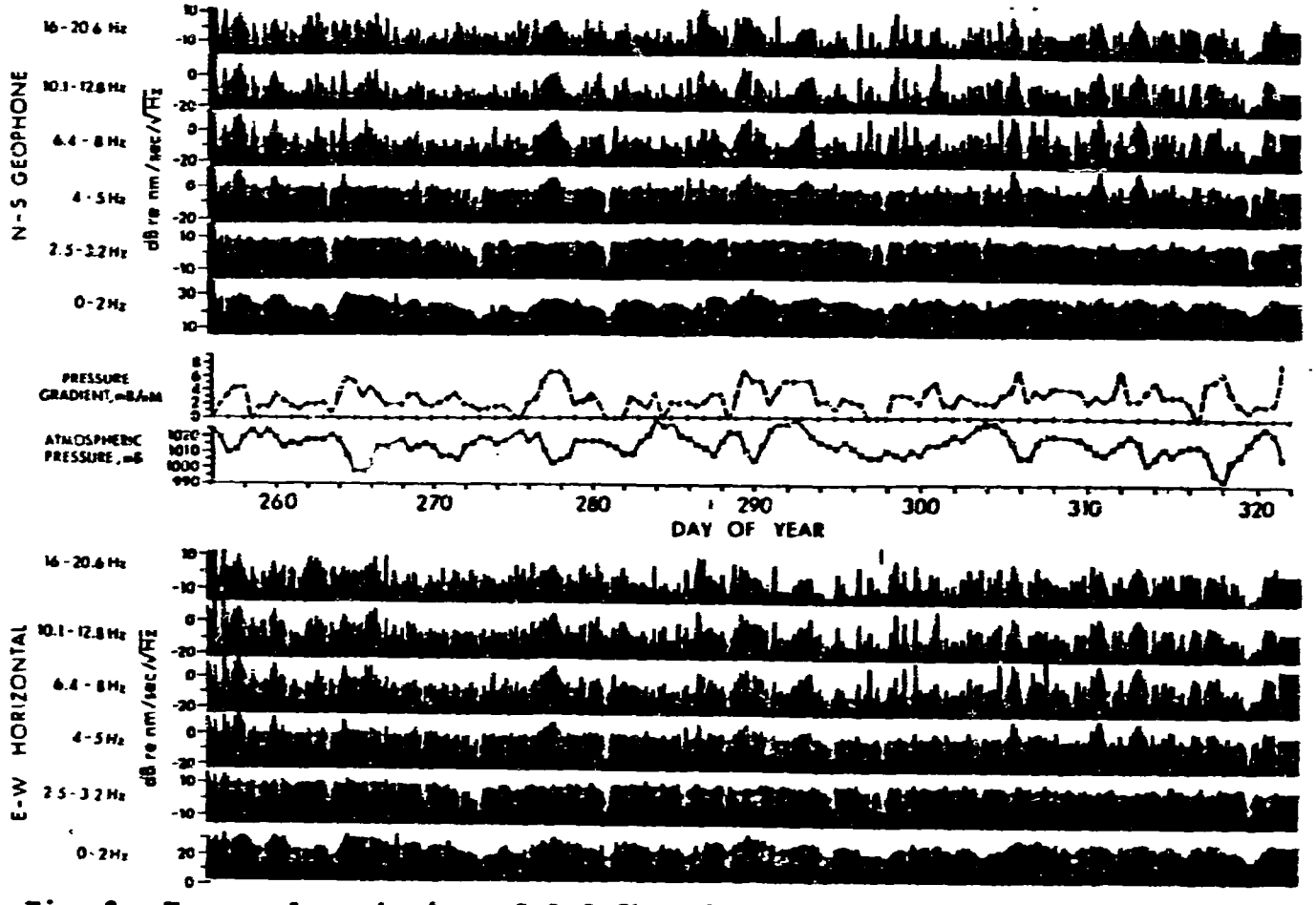

Fig. 2. Temporal variation of 088 IV noise levels over the 64-day recording period in 1982. The top six traces are noise levels in 1/3 octave filters recorded by the N-S geophone, and the bottom six were recorded by the E-W geophone. The middle two traces were obtained from atmospheric 12-hour weather maps at the drill site. Note that noise peaks at the higher frequencies correlate well with high pressure gradients, and low noise levels at low frequencies appear to correlate with high atmospheric pressure and low gradients.

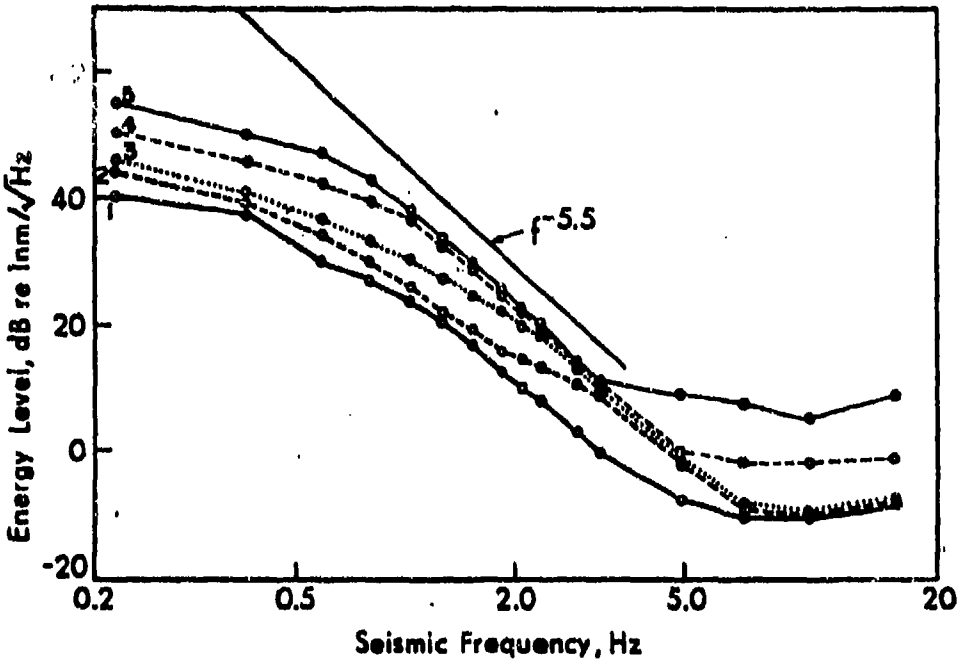

Fig. 3. Horizontal geophone noise levels on OBS IV during a storm beginning on day 263, 1982. Each line represents noise level at 6 hour intervals increasing in time from the lowest curve to the highest. A curve with a slope of $f^{-5.5}$ is shown for reference. Note that a noise level saturates at lower and lower frequencies as the storm progresses.

0.5 to 5 Hz on both the ocean floor and below the ocean floor in two different storms by instruments far from any land implies that the mechanism may not be dependent on interaction of waves traveling in different directions, but on the sea state itself. The energy in the pressure field is proportional to the square of the amplitude of the ocean wave, thus the seismic noise spectrum may yield a direct measure of wave heights. The saturation level is easy to identify from its spectral slope of $f^{-5.5}$. This level is important because it implies a constant source energy in deep water and may be useful for calibration purposes.

SHIPPING NOISE: Signals from passing ships are identified in Figure 2 by the relatively narrow band spikes lasting from four to ten hours. More than 130 signals of this type are identified during the 6.4-day period, and ship signals dominate the noise spectrum above 5 Hz for some time periods. Because of the directional nature of the geophones, the direction to a ship can be determined (with a 180^{o} ambiguity) and its distance if its speed is known[4].

BIOLOGICAL NOISE: A persistent bi-frequency noise source at about 17 and 20 Hz is commonly observed in the borehole data. The signals from this "whale" have a peak level about 20 dB above noise level, and often are heard for days at a time from more than one source. Signals observed are identical to those observed on hydrophones in the Pacific[4,8].

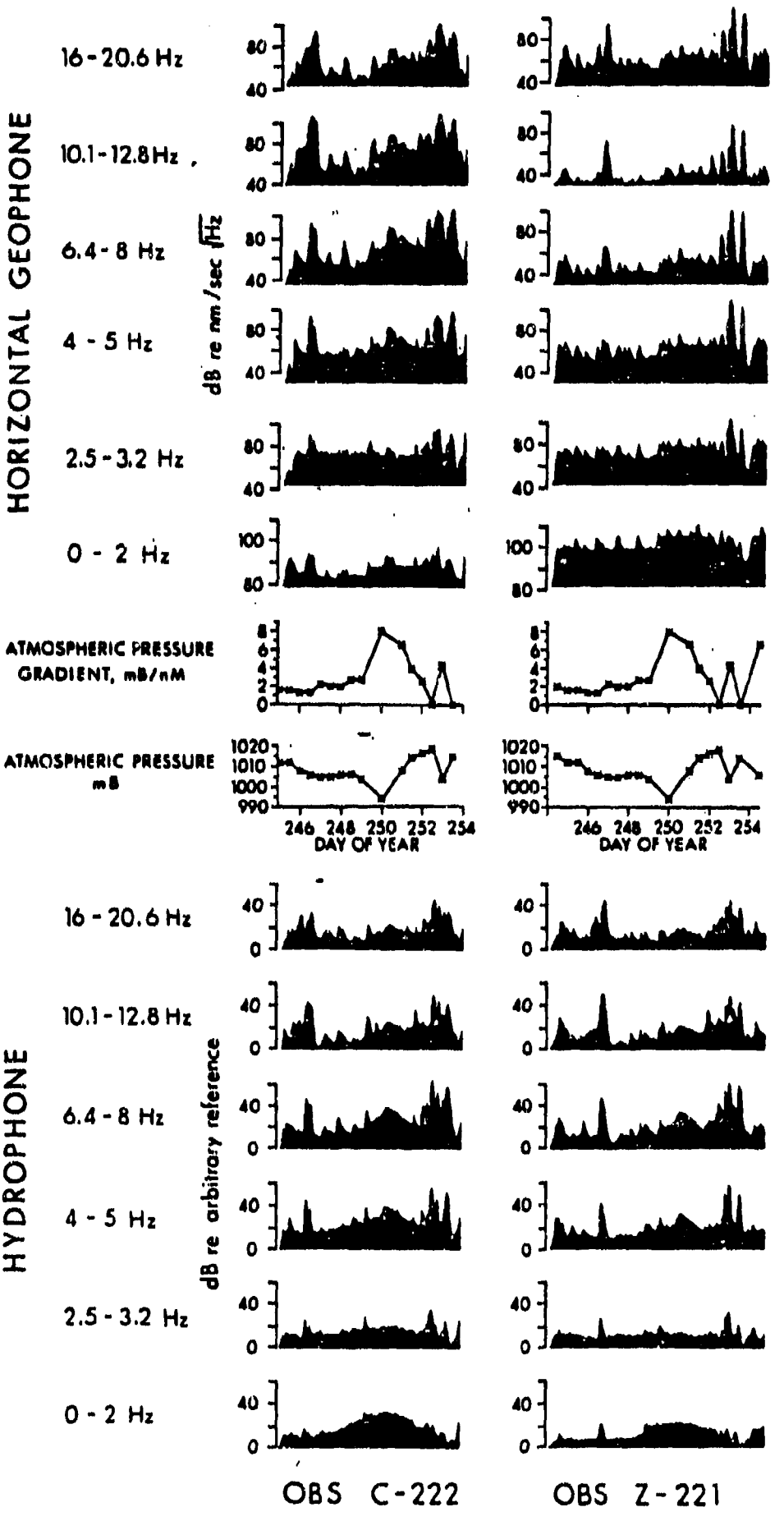

Fig. 4. Temporal variations of OBS noise levels over about eleven days in Sept. 1982 at the OSS IV site. See Figure 2 for details. OBS C-222 was about 40 km south of the site and Z-221 was at the site.

A plot similar to Figure 2 is shown in Figure 4 for two eleven-day periods recorded by two ocean bottom seismometers just before the time period shown in Figure 2. Nearly all the noise fluctuations correlate with known activities during the experiment (Figure 5). A tropical cyclone (Hurricane Gordon) passed the site on day 250, 1982, and its effects are noticeable on both OBSs, especially on the hydrophones, but at a signal-to-noise level less than observed for similar storms recorded on the borehole system. The increase in noise level above 5 Hz during the storm is larger on the horizontal geophone than on the hydrophone (Figure 6), an observation also noted by Bradner[9] in mid-water experiments. In Figure 6, the change in noise spectra withtime are plotted for 24 hour intervals from the calm period prior to Hurricane Gordon until its peak. Note that the $f^{-5.5}$ saturation slope is observed on the horizontal geophone. The slope of saturated noise on the hydrophone traces is different because the hydrophone traces are not corrected for instrument response. Note also that, except for sources identified with the experiment, few ship sources are visible. The noise level of the horizontal geophones are 40 dB, or more, greater than the levels of the borehole geophones. This increased noise is caused by trapping and amplification of shear waves in the low velocity sediments, and by Stoneley waves.

CONCLUSIONS

Noise levels in a deep-ocean borehole between 0.2 and 5 Hz are controlled completely by sea state. Above 5 Hz, noise levels increase during storms because of breaking waves but are otherwise controlled by either shipping or biological noise. Placement of seismic sensors in a borehole extending into basement increases the sensitivity to ocean acoustic sources because of reduced noise levels relative to the ocean floor. Signal-to-noise improvement is difficult to quantify with the data in-hand, but it appears to be more than 6 dB at frequencies above 5 Hz.

ACKNOWLEDGMENTS

This research was funded by the Office of Naval Research. Preparation of figures, typing, review and editing by R. Rhodes, K. Rehbock, and Rita Pujalet are gratefully acknowledged. Hawaii Institute of Geophysics Contribution No. 1609.

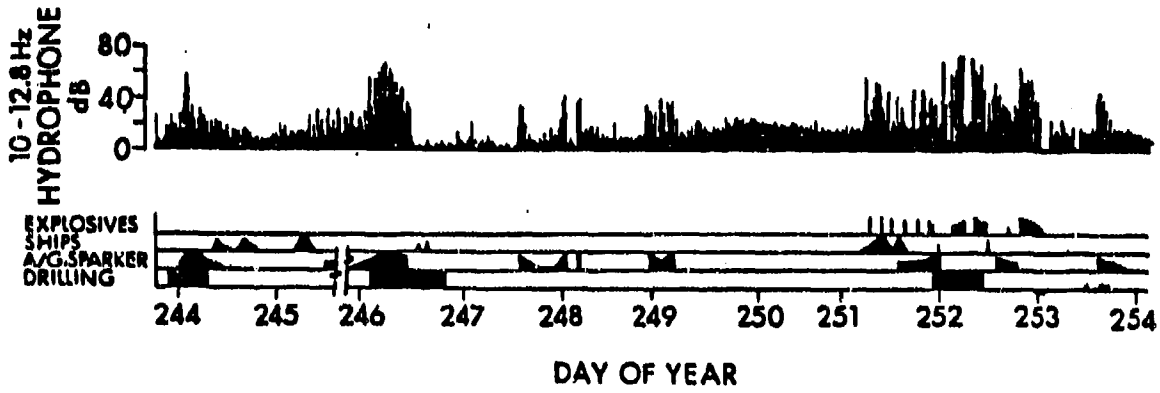

Fig. 5. Correlation of known activities with noise levels on an OBS (Z-221) at the OSS IV site.

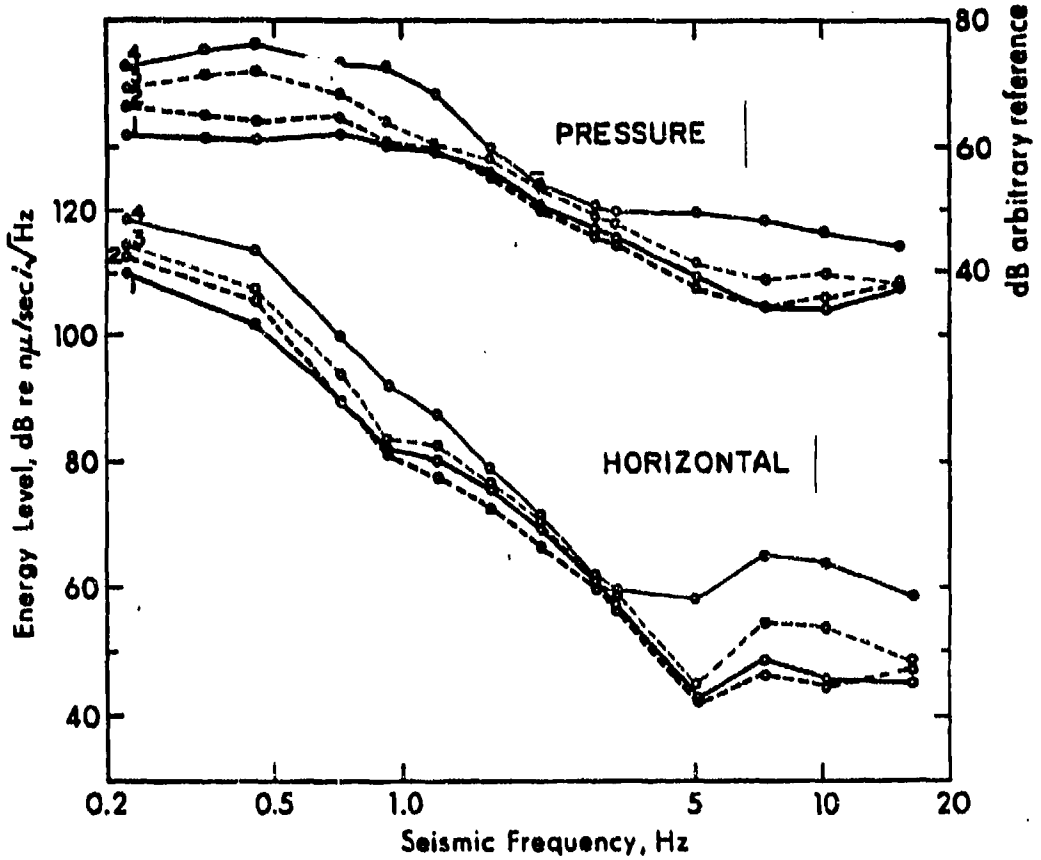

Fig. 6. Change in noise level of OBS C-222 with time (24 hour intervals) before and during hurricane Gordon beginning on day 248, 1982. Each curve represents the noise spectrum at a different time.

1. Byrne, D. A., D. Harris, F. K. Duennebier, and R. K. Cessaro, Technical Review of the Ocean Subbottom Seismometer System Installed in Deep Sea Drilling Project Site 581C, Leg 88, in Init. Repts. of the Deep Sea Drill. Proj., Vol. 88, in press (1985).
2. Anderson, P., and F. K. Duennebier, Orientation of Horizontal Ocean Bottom Seismic Sensors from Explosive Data, in preparation (1985).
3. Phillips, O. M., The Dynamics of the Upper Ocean, Cambridge Univ. Press, 113-114 (1969).
4. Duennebier, F. K., C. McCreery, D. Harris, R. K. Cessaro, C. Fisher, P. Anderson, OSS IV: Noise Levels, Signal-to-Noise Ratios, and Noise Sources, in Init. Repts. of the Deep Sea Drill. Proj., Vol. 88, in press (1985).
5. Longuet-Higgins, M. S., A Theory on the Origin of Microseisms, Phil. Trans. London. A, 243:1-35 (1950).
6. Haubrich, R. A., W. H. Munk, F. E. Snodgrass, Comparative Spectra of Microseism and Swell, Bull. Seism. Soc. Amer., 53:27-37 (1963).
7. Bernard, Pierre, Short Review and Recent Results on Microseisms, Geophys. Surveys, 5:395-407 (1983).
8. Northrop, J., W. C. Cummings, M. F. Morrison, Underwater 20 Hz Signals Recorded Near Midway Island, J.A.S.A., 49: 1909-1910 (1971).
9. Bradner, H., Microseism Propagation via Oceanic Waveguide, Pure Appl. Geophys., 103:266-273 (1973).

DETERMINING THE ORIENTATION OF HORIZONTAL OCEAN BOTTOM SEISMIC SENSORS FROM EXPLOSIVE CHARGES

by

P. N. Anderson

F. K. Duennebier

R. K. Cessaro

Hawaii Institute of Geophysics, University of Hawaii

2525 Correa Road, Honolulu, Hawaii 96822, U.S.A.

Abstract

High quality, three-component seismic data has been obtained from an ocean sub-bottom seismometer (OSS) emplaced in a drillhole beneath the ocean floor. Future experiments involving similar instruments, as well as three-component ocean bottom seismometers (OBSs), will require azimuthal orientation of the two orthogonal horizontal geophone axes in addition to orientation of the vertical axis. We have determined the azimuthal orientation of the horizontal axes of OSS IV to within $\pm 1.5^{\circ}$ by analysis of first arrivals from 23 explosive charges fired to the downhole instrument for refraction experiments. This accuracy should be sufficient for most experiments, and requires no extra instrumentation or effort during emplacement.

Introduction

A lack of ocean-floor seismic data recorded by seismographs containing three orthogonal geophones, poor coupling, and low signal-to-noise ratios common in much ocean bottom seismometer data, have led to development and emplacement of several sub-bottom instruments over the last few years. An ocean sub-bottom seismometer (OSS IV), designed and built at the Hawaii Institute of Geophysics, was emplaced from the D/V Glomar Challenger into Hole 581C on DSDP Leg 88 in September, 1982 (Byrne et al., in press). Hole 581C is located in the northwest Pacific (43.9240°N., 159.7973°E.) in 110-m.y.-old ocean crust covered by 358 meters of sediment and 5467 meters of water. The instrument was clamped against the side of the drillhole 21 meters below the sediment-basalt interface (Figure 1). The OSS IV detects particle velocity on three orthogonal, 4.5 Hz geophones, and also records temperature and horizontal tilt. Explosive charges were fired and recorded during a refraction experiment conducted shortly after emplacement. In addition, a continuous sixty-four day record of earthquake, ship and biological signals was recovered from OSS IV nine months after emplacement (Duennebier et al., in press).

In order to make optimal use of these data, the orientation of the three geophone axes have been determined. The "verticality" of the vertical sensors is not critical, as shake table tests of the vertical sensors show less than 1 dB variation in output response to vertical velocity over a tilt range of almost 20°, and the tilt of the vertical sensors (located in a pad pressed against the side of the hole) is certainly less than 5°. The tilt sensors are used to determine the tilt of the plane containing the horizontal sensors. Both tilt sensors registered within 1 degree of horizontal. Azimuth sensors for borehole use are expensive and require

additional telemetry and space, therefore, none were included in the OSS. It was expected that the azimuths of the horizontal sensors could be determined from records of explosive charges fired at known azimuths and distances from the instrument. Future plans for well-coupled, three-component borehole and OBS experiments require knowledge of the sensor azimuths, the accuracy with which the azimuths are known, and sources of possible error. We will show that the azimuthal orientation of the OSS IV horizontal geophones can be determined to within $\pm 1.5^{\circ}$ by analysis of shots fired for refraction experiments. Underlying assumptions are that the shot positions are accurately known and that geophone sensitivities are well matched. Also, we will show that we can take advantage of the azimuths determined to better locate the OSS and nearby shots.

Procedure

Twenty-three shots selected for this study are distributed about a circle at a radius approximately 4.5 km from the OSS (Figure 2). The orientation method presented can be applied to any pattern of shots, but azimuthally well distributed shot patterns are most desirable for increasing the accuracy of the procedure and for identification of possible site-dependent error sources such as anisotropy or underlying structure (Duennebier and Anderson, this issue).

Comparison between the amplitudes of a particular arrival sensed by each of the two horizontal geophones can be used to determine the azimuth of that arrival relative to the geophone axes. This is possible because OSS IV contains two well-matched, orthogonal, horizontal geophone pairs. Each geophone is sensitive to the particle velocity component parallel to its axis. The amplitude of an arriving signal recorded on either of the

horizontal geophones varies directly with the cosine of the angle between the particle velocity vector and the geophone axis. (I.e., There is an inverse relationship between the amplitude of the recorded signal and the angular separation between the particle velocity vector and the geophone axis.)

During the refraction experiment, data from the OSS IV geophones were digitally recorded at a rate of 100 samples/sec. During processing, the first 10 samples of each arrival were used as a "first motion" time series for each of the horizontal channels. The signal amplitudes from each of the two orthogonal horizontal channels were then plotted as (X,Y) pairs on a plane. The resulting graphs represent particle velocity with respect to the axes of the horizontal geophones (Figure 3a). A best-fit straight line approximation of the particle velocity was found for the first arrival from each shot, and the azimuth of the best-fit line was calculated relative to the H1/H2 coordinate axes. The azimuth of the best-fit line for one example, shot #625, was determined to be 57° (Figure 3b).

In a homogeneous, isotropic, horizontally layered media each compressional wave arrival should cause particle motion in the horizontal plane parallel to a line between source and receiver. Therefore, the azimuth of the line of best fit (Figure 3) is taken as the azimuth of the shot relative to the OSS geophone axes (referencing one sensor as + south and the other as + east). The azimuth of the shot from the OSS relative to true north is known from ship's navigation. Therefore, it is possible to determine the azimuthal orientation of the geophones. The angle found by taking the difference between the azimuth of the shot from the OSS relative to true north (known from ship's navigation) and the azimuth of the shot relative to the OSS geophone axes will be referred to as azimuth rotation

(Figure 4a) and represents the angle of rotation from true north of the downhole instrument in the drillhole. A plot of azimuth rotation vs. azimuth relative to north for a series of shots should define a horizontal straight line (Figure 4b). The intersection of that horizontal line with the vertical axis of the plot (azimuth rotation) marks the number of degrees of rotation of the horizontal geophones from true N/S-E/W alignment. It is possible to use this procedure using either first arrivals, as discussed here, or direct (water wave) arrivals (Figure 3c,d).

Scatter of points on rotation vs. azimuth plots may be produced by noise in the data, interference with other arrivals, local anomalous structure or navigational errors associated with shot or sensor location. Scatter caused by any of these factors should be considered a source of azimuth error since it contributes to error in azimuth rotation. Random navigational errors and noise will tend to cause random errors in azimuth rotation angles. However, azimuth error produced by some factors is sufficiently systematic to produce a sinusoidal pattern in azimuth rotation data plotted as a function of azimuth. Anisotropy or unmatched sensors will produce a two-cycle sinusoidal pattern over 360°. A single-cycle sinusoidal pattern over 360° may be attributed to inaccurate sensor location relative to shot position or a sloping sediment-basement interface where refracted P-wave arrivals are used for the analysis (Duennebier and Anderson, this issue).

The data in Figure 5a show the presence of a single-cycle sinusoidal pattern in the rotation vs. azimuth data. The azimuth error producing this pattern may be due to inaccurate sensor location or to a sloping sediment-basement interface. A dipping sediment-basement interface may be ruled out

as the cause of the sinusoid pattern because reflection profiles in the area clearly show a nearly horizontal basement surface.

The remaining possibility for a single cycle pattern is inaccurate sensor location. Inaccurate sensor location will cause azimuth errors for all shots except those along the line through the actual sensor location and the incorrect sensor location (Figure 6). Systematic error in shot location will produce the same sinusoidal effect as error in sensor location, however, the single-cycle sinusoidal pattern present in Figure 5a is also present in our data when arrivals from shots lying on other refraction lines are examined. It is extremely unlikely that such a uniform error in navigation would exist over such a large number of shots, and we therefore attribute the sinusoidal pattern to an error in the location of Hole 581C.

A linear regression fit of a sine curve (restricted to 1 cycle in 360°) to the data points is shown in Figure 5a. The curve shows a maximum amplitude of 6.5° and inflection points at 91° and 271°. The inflection points indicate that the azimuth error of shots east and west of the OSS position is nearly zero. while the maximum azimuth error (6.5°) occurs for shots lying north and south of the receiver . Relocation of the OSS must be to the west in order to reduce the angle of azimuth error for shots lying north or south of the receiver (Figure 6). The amplitude of the sine curve is used to calculate the distance which the hole should be moved. For shots at 4.5 km, calculations show that relocation of the receiver approximately 500 meters to the west will reduce the amplitude of the sine curve to zero. The location of the Glomar Challenger during drilling of the hole is very accurately known from numerous satellite fixes obtained during drilling and it was assumed that the hole was directly under the ship. However, displacement of the hole by 500 meters is less than 10% of the water depth

in which the drilling took place. Displacement of the drill string by this amount is not unreasonable, although difficult to prove. In support of this conjecture Figure 5b shows a replotted version of the data in Figure 5a using the relocated drillhole position. The data are now much more closely approximated by a straight line fit and the amplitude of the sinusoidal pattern has been reduced to nearly zero. The corrected location of hole 581C by this analysis is 43.9240°N., 159.7909°E.

Three of the shots have noticeably poor correlation with the sinusoidal pattern in Figure 5a. The shots lie approximately 180° apart (northwest and southeast of the receiver, Figure 2). An examination of the topography of the sediment-basalt interface reveals a narrow, linear, sediment-filled, depressional feature trending northwest-southeast through the OSS site (Figure 2). The shots least well approximated by the sine curve (shots 602, 617, and 618) are also most closely aligned with this trough-like feature. The particle motion associated with the refracted first arrivals from each of these shots is distorted from alignment with receiver and shot position because the first arrival has travelled "off-line" through the shallow, higher velocity basement to either side of the trough. The three shots identified were disregarded in order to obtain a better estimate of error.

The mean azimuth rotation of the remaining data points was determined, at a level of confidence of 95%, to be within ±1.5° of -1.0°. Therefore, based on an initial assumption that one sensor is oriented with positive output south, and the other sensor is oriented with positive output east, we have found that the instrument is rotated so that the first sensor is oriented with positive output at 89.0° and the second sensor is oriented with positive output at 179.0° (i.e. the number of degrees by which the

horizontal axes of the downhole instrument are rotated with respect to north is within $\pm 1.5^{\circ}$ of 1.0° counterclockwise).

The procedure outlined above was also used for direct (water wave) arrivals from the same set of shots. The sinusoidal pattern was removed in the same manner, and the mean azimuth rotation was found, at a level of conidence of 95%, to be within $\pm 3.9^{\circ}$ of -4.6° from true north. The mean of the first arrival rotations lies within the 95% confidence limits for the mean of the water wave rotations.

The standard deviation of the azimuths for first arrivals calculated by this procedure is 3.2°. Therefore, the azimuth from the OSS for any particular shot can be determined within $\pm 6.7^{\circ}$ at a confidence level of 95%. This level of accuracy will provide a sufficiently narrow "window of confidence" for relocation of those shots lying near enough to the hole. Relocation may be accomplished on the basis of travel time and azimuth to the shot as calculated here. Preliminary results suggest that these relocations give superior results to the initial shipboard shot locations for shots within a few km of the hole (Duennebier and Anderson, this volume). The "window of confidence" will be too wide to allow improvement of shipboard shot locations for shots at greater distances.

The azimuths of the water wave arrivals were determined with a standard deviation of 8.8°. The greater dispersion of the azimuths for water wave arrivals may be attributed to interference from other arrivals present in the data at the same time as the arrival of the water wave. The inherent advantage to using water wave arrivals for this analysis is that they are unaffected by anisotropy or topographic and structural variation. However, this advantage is offset by the fact that the water wave is a later arrival and mixed with other arrivals. As expected, analysis of water wave

arrivals does not indicate dependence on basement topography (as analysis of the P waves does) since water wave travel paths are not refracted through the crustal material.

Conclusions

The method outlined here offers an inexpensive and accurate way to obtain azimuthal orientation of horizontal geophones in downhole seismometers and three component OBSs. Analysis of first arrivals from azimuthally well distributed shots fired to the downhole seismometer OSS IV indicate with 95% certainty that the horizontal geophone axes are within $\pm 1.5^{\circ}$ of a 1.0° counterclockwise rotation from the N/S-E/W coordinate system. Consistent results were also obtained from analysis of the more error-prone water wave arrivals.

The accuracy of this method is limited by the accuracy with which instrument and shot positions are known. Accuracy may be improved by use of closer shot spacing and the use of more exact navigation systems (such as GPS - global positioning system). Analysis of systematic errors (Duennebier and Anderson, this issue) may yield improved sensor locations and possible information on crustal anisotropy. We find, from our analysis, that the instrument in Hole 581C is actually displaced 513 meters to the west of the location of the Glomar Challenger during drilling.

The generally horizontal topography of the sediment-basement interface in the vicinity of this particular downhole seismometer allows us to use first arrival information to orient the horizontal geophone axes to within $\pm 1.5^{\circ}$. However, water wave arrivals are likely to provide the most accurate information for sensor orientation in structurally more complex areas because their direction of propogation is not so susceptible to distortion

from anomalous structure below the ocean floor. Use of water wave arrivals suffers from error produced by other arrivals present at the same time as the water wave.

Azimuths of individual P waves arriving at OSS IV can generally be determined (at a confidence level of 95%) with an accuracy of about $\pm 6.7^{\circ}$. This is thought to be accurate enough for relocation of shots close to the hole based on their travel times and azimuths.

Use of the method presented here on data obtained from well-coupled and well-matched three-component ocean bottom seismometers or borehole seismometers makes determination of the orientation of seismic sensors both possible and practical. Directivity studies can then proceed with knowledge that the receiving instrument is oriented with a known degree of precision.

References

Byrne, D. A., D. Harris, F. K. Duennebier, and R. K. Cessaro, Technical review of the ocean subbottom seismometer system enstalled in deep sea drilling project site 581C, leg 88, in Initial Reports of the Deep-Sea Drilling Project, 88, edited by F.K. Duennebier, in press, U.S. Government Printing Office, Washington, D.C., 1985.

Duennebier, F. K. and P. N. Anderson, Factors producing error in orientation of horizontal ocean bottom seismic sensors, This volume.

Duennebier, F. K. and J. G. Blackinton, The ocean subbottom seismometer, in Handbook of Geophysical Exploration at Sea, Geyer, R.A. (Ed.), Boca Raton, Florida, (CRC Press), pp 317-332.

Duennebier, F. K., C. S. McCreery, D. Harris, R. K. Cessaro, C. Fisher, and P. N. Anderson, OSS IV: Noise levels, signal to noise ratios, and noise sources, in Initial Reports of the Deep Sea Drilling Project, 88, edited by F. K. Duennebier, in press, U.S. Government Printing Office, Washington, D.C., 1985.

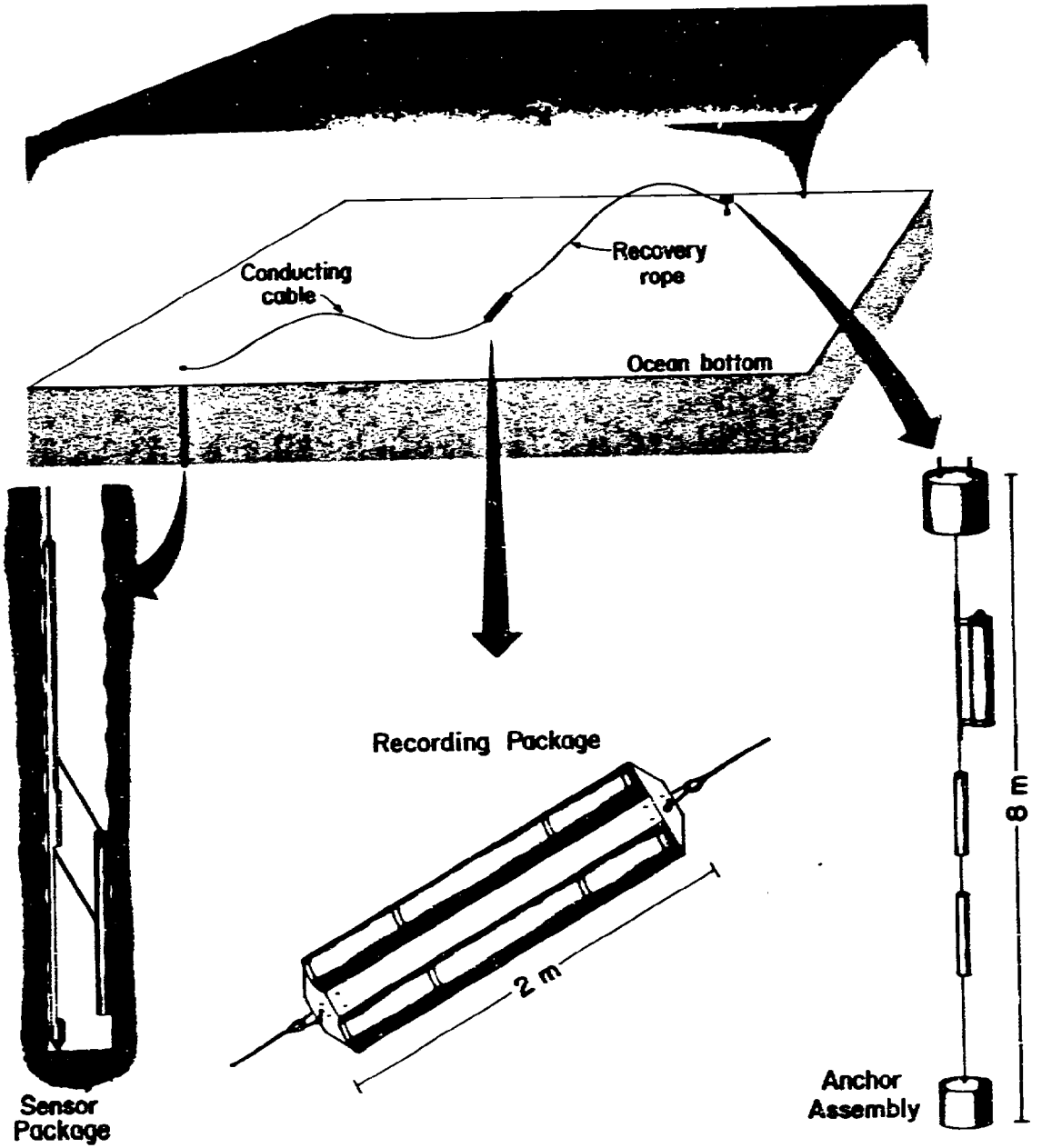
Conducting cable
Recovery rope
Ocean bottom
Recording Package
2 m
8 m
Sensor Package
Anchor Assembly

FIGURE 1

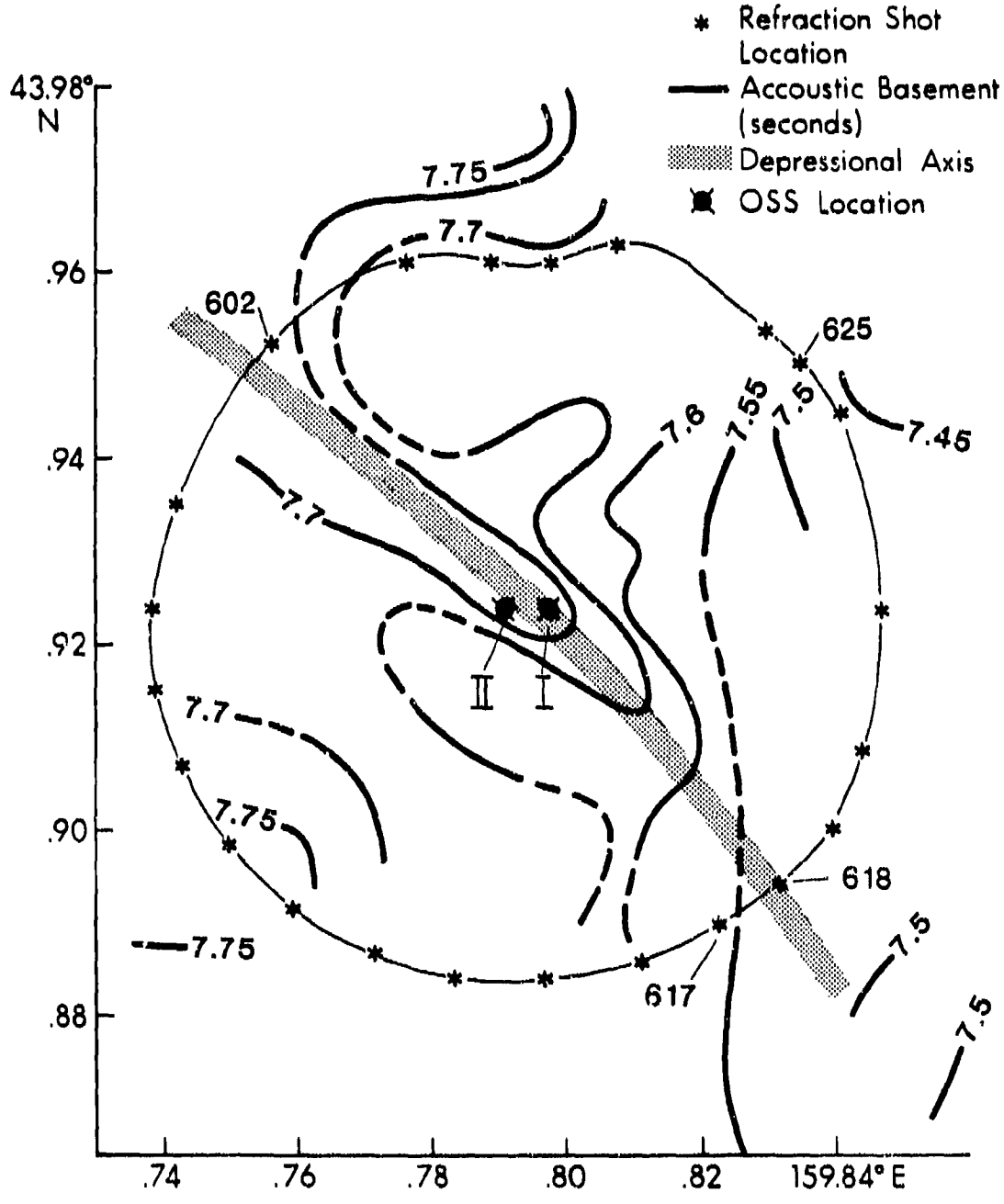
Refraction Shot Location
Accoustic Basement (seconds)
Depressional Axis
OSS Location
43.98° N
.96
.94
.92
.90
.88
.74
.76
.78
.80
.82
159.84° E
602
625
618
617
7.75
7.7
7.6
7.55
7.5
7.45
II
I

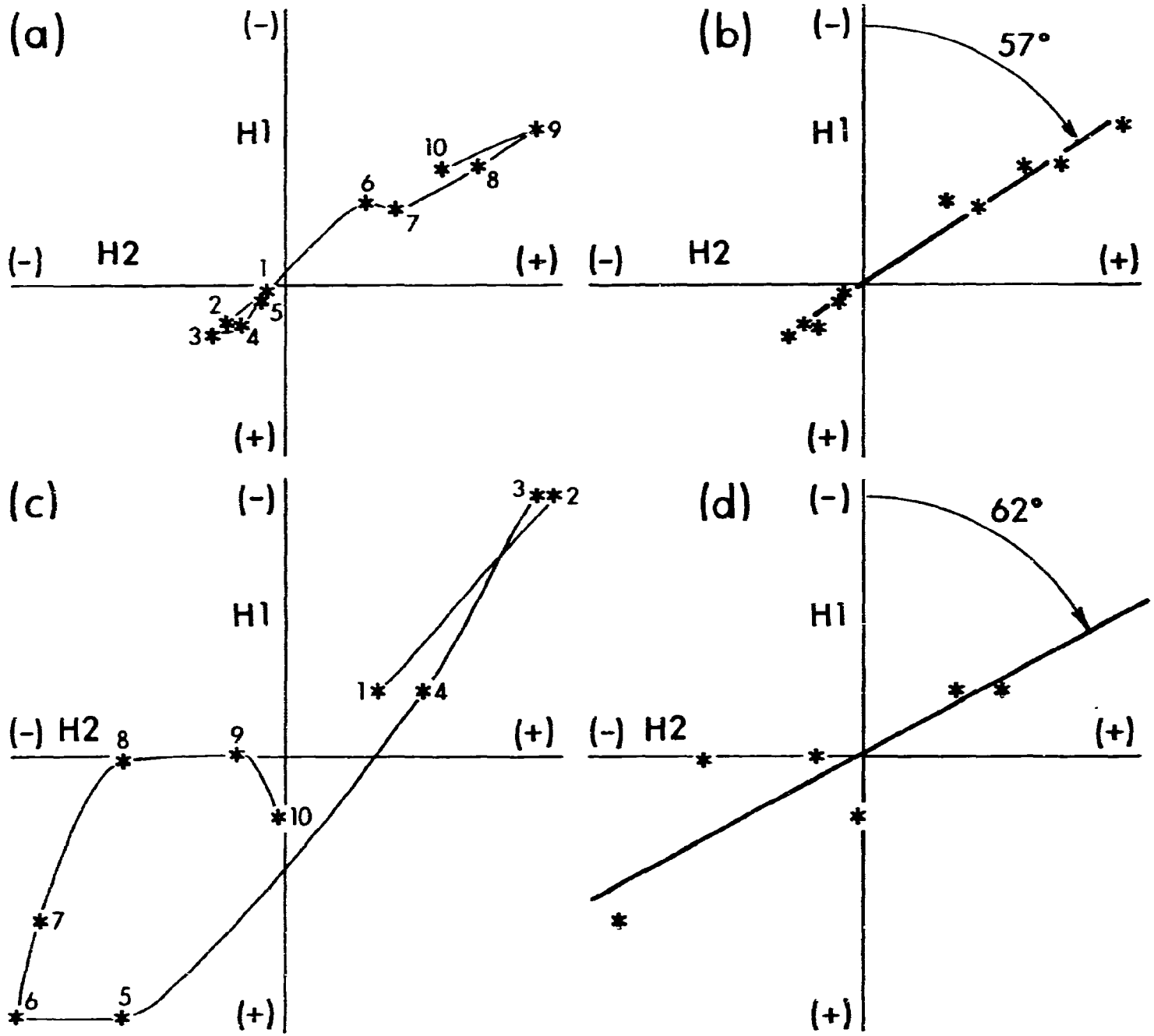

Figure 3

(a)

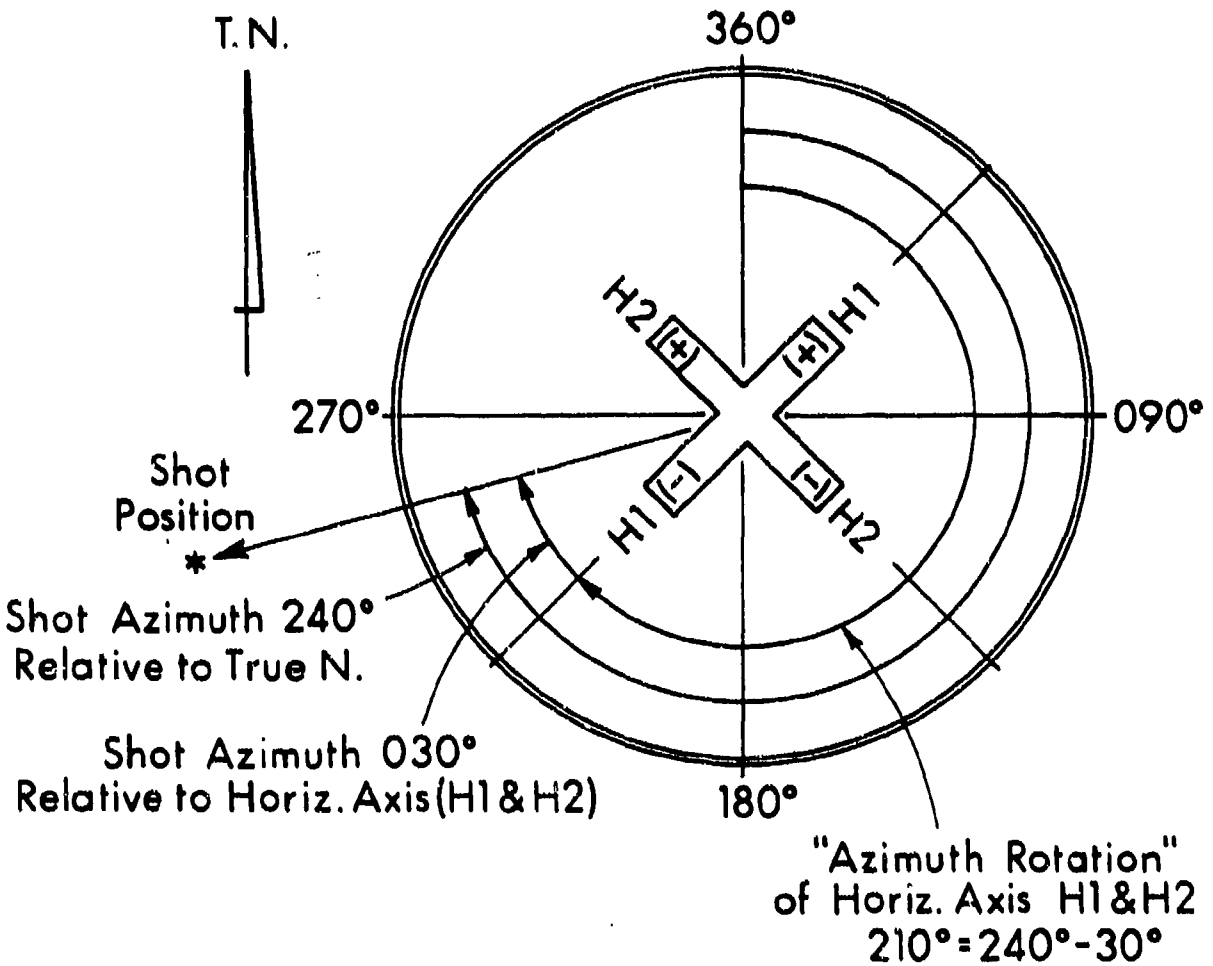
T.N.
360°
270°
090°
180°
H2
(+)
H1
(+)
H1
(-)
H2
(-)
Shot
Position
*
Shot Azimuth 240°
Relative to True N.
Shot Azimuth 030°
Relative to Horiz. Axis (H1 & H2)
"Azimuth Rotation"
of Horiz. Axis H1 & H2
210° = 240° - 30°

Figure 4a

(b)

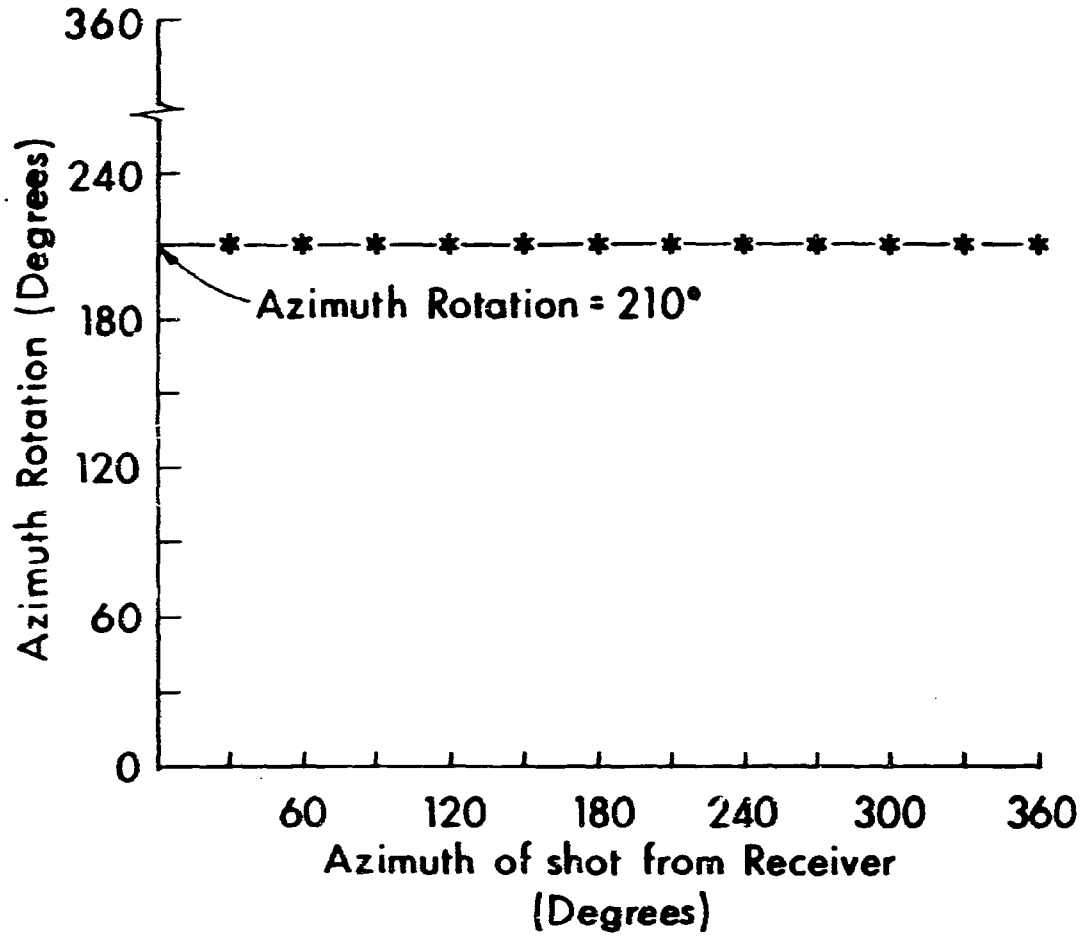
360
240
180
120
60
0
Azimuth Rotation (Degrees)
Azimuth Rotation = 210°
60
120
180
240
300
360
Azimuth of shot from Receiver
(Degrees)

FIGURE 46

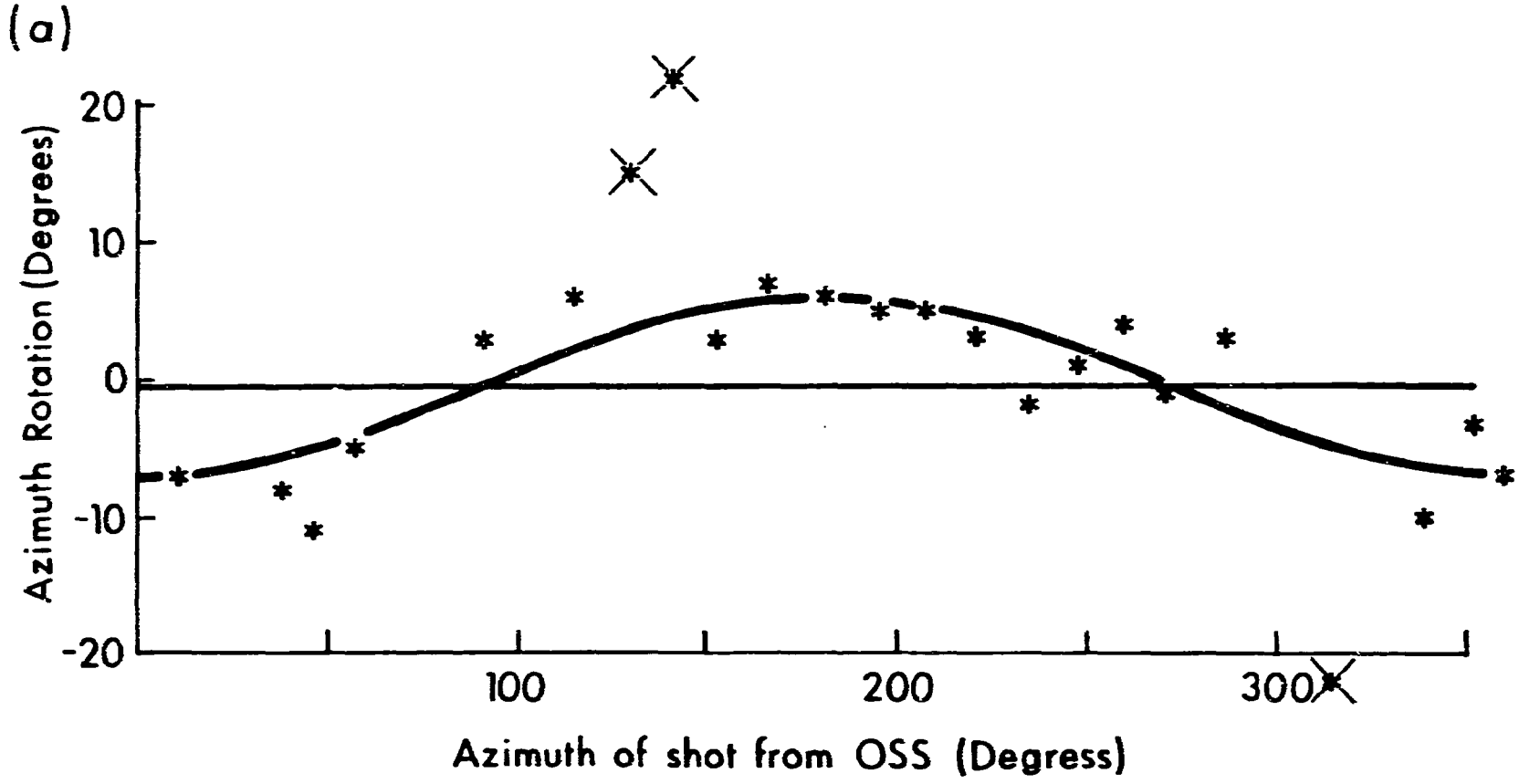
(a)
20
10
0
-10
-20
Azimuth Rotation (Degrees)
100
200
300
Azimuth of shot from OSS (Degress)

(b)

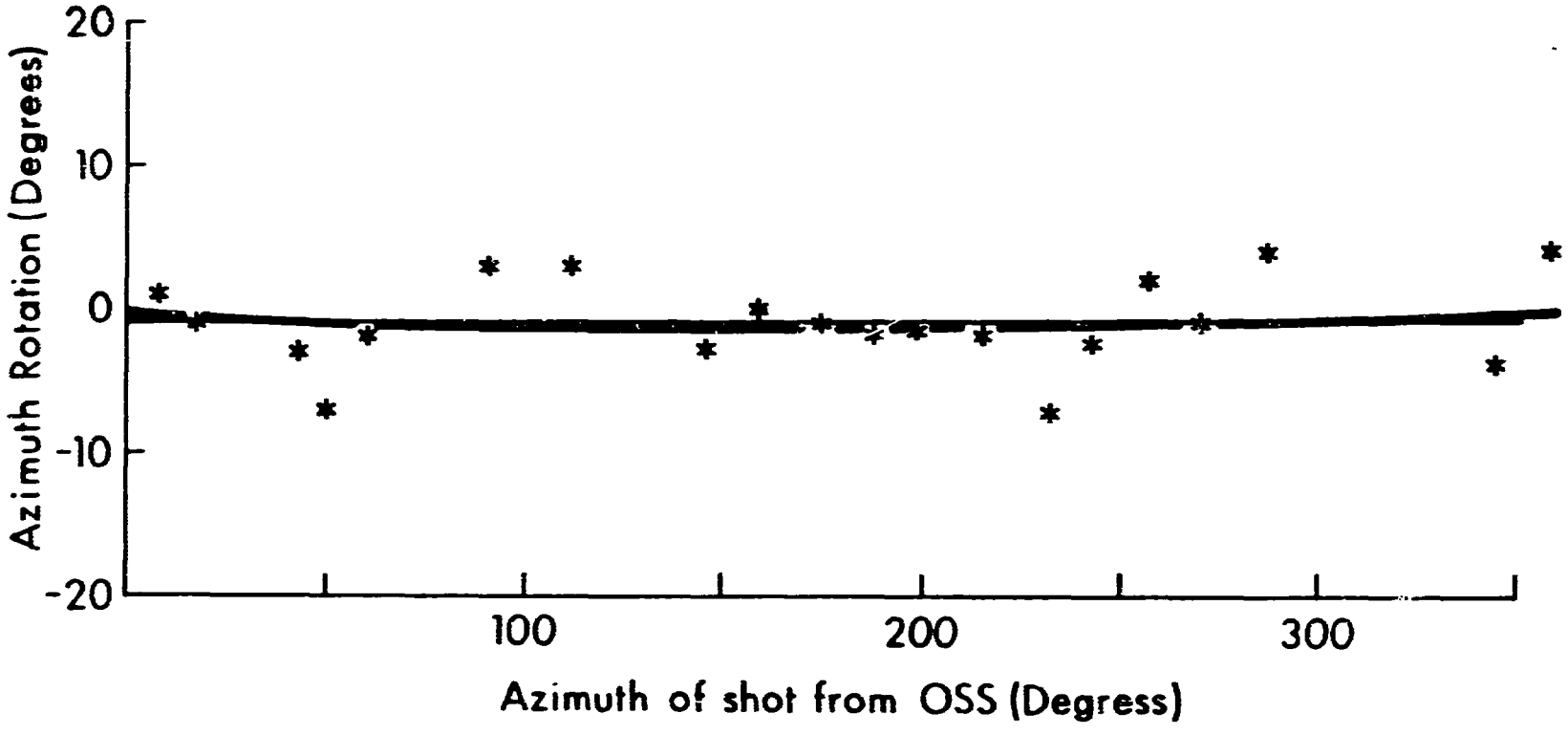
20
10
0
-10
-20
Azimuth Rotation (Degrees)
100
200
300
Azimuth of shot from OSS (Degress)

FIGURE 56

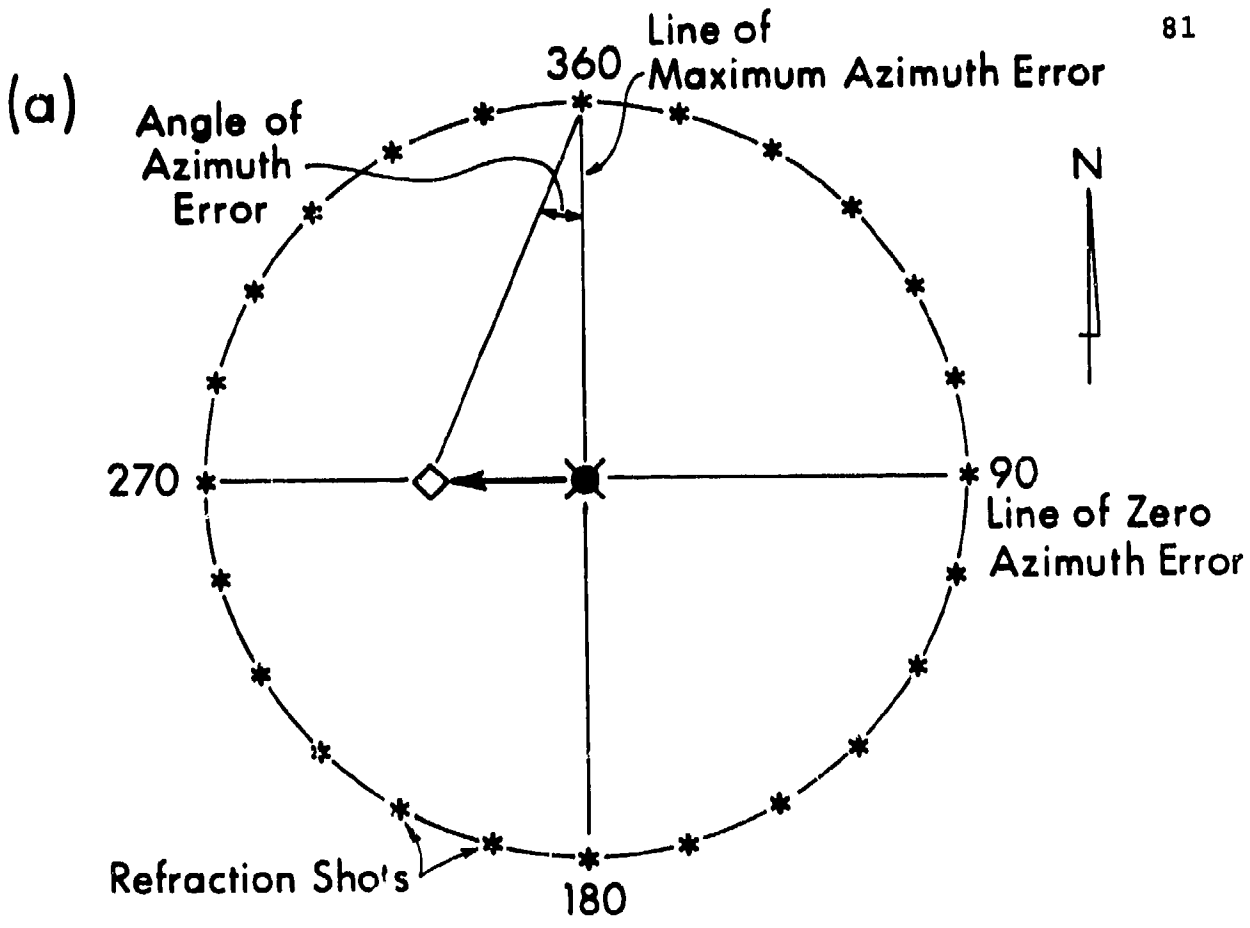
(a)
360
Line of
Maximum Azimuth Error
Angle of
Azimuth
Error
N
270
90
Line of Zero
Azimuth Error
Refraction Shots
180

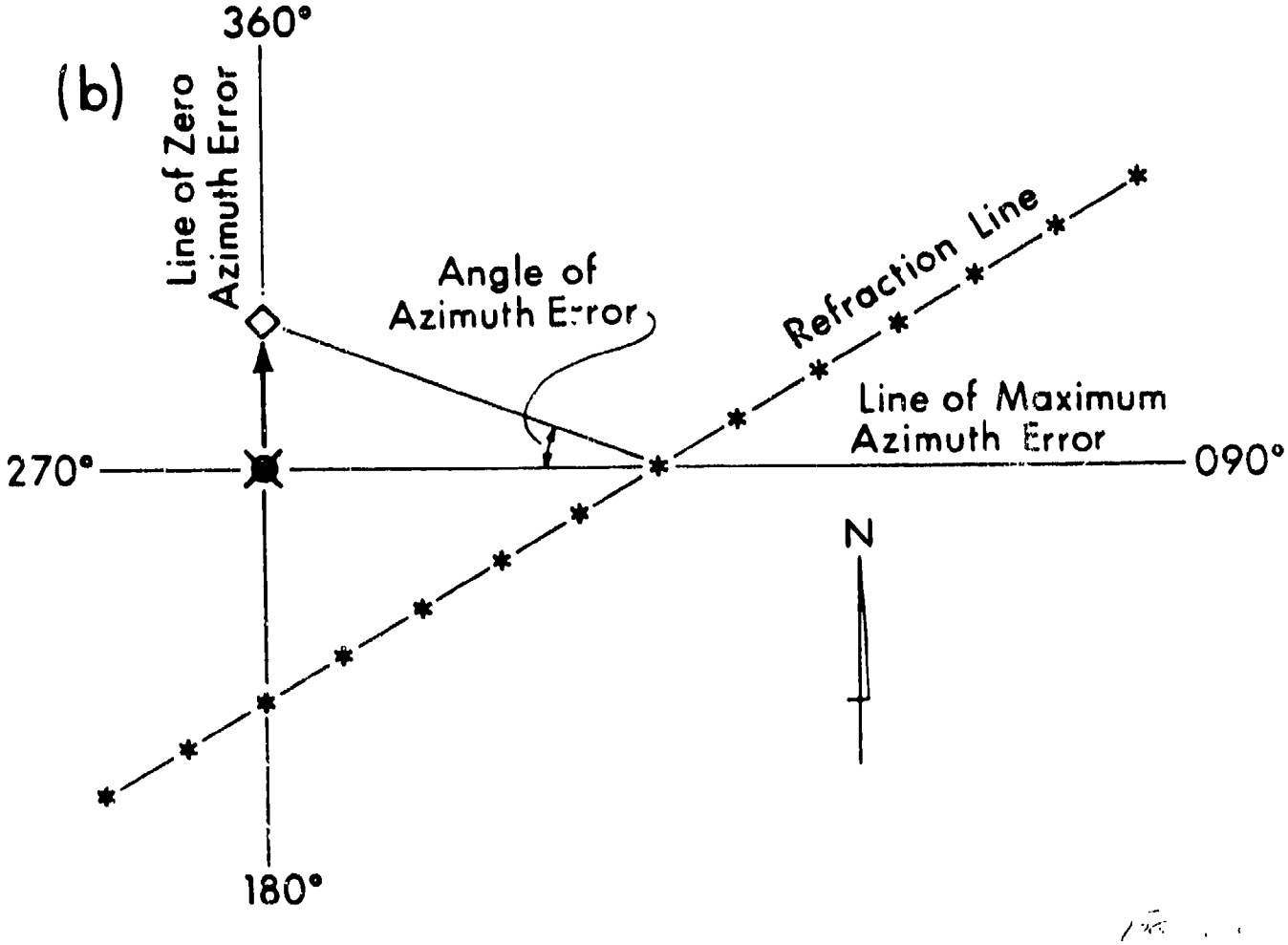
(b)
360°
Line of Zero
Azimuth Error
Angle of
Azimuth Error
Refraction Line
Line of Maximum
Azimuth Error
270°
090°
N
180°

Figure 1. The ocean subbottom seismometer system. The borehole package is emplaced in a deep sea drill hole with power transferred to it, and data sent from it, through a conducting cable connected to a recording package. The recording package is attached to a floating rope that is in turn connected to a float-anchor assembly for recovery (from Duennebier and Blackinton, 1983).

Figure 2. Shot positions, OSS position (I), and relocated OSS position (II) are shown superimposed on bathymetry of the acoustic basement (contour interval = .05 sec). Note linear, sediment-filled depression trending NW-SE through the OSS position.

Figure 3. (a). An example (shot #625, Figure 2) of first arrival particle velocity relative to the horizontal geophone axes (referencing H1 as + south and H2 as + east). The plot axes represent amplitude of the arriving signal as recorded by each of the horizontal sensors (H1 and H2). The first 10 samples (*) of the arrival from each horizontal channel (H1 and H2 were used to establish this "first motion" time series. (b). The straight line best fit to the particle velocity yields an azimuth of 57° relative to the geophone axes for shot #625. (c). Particle motion of the water wave arrival from shot #625. Note that the high amplitude of the water wave arrival has resulted in clipping at some sample points (2,3,5 and 6). These points were not used for establishing the line of best fit. (d). The line of best fit for the water wave particle velocity yields an azimuth of 62° for shot #625. The difference between the water wave results and the first arrival results in (b) can be attributed to interference from other arrivals present in the data at the same time as the water wave.

Figure 4. (a). H1 and H2 depict the horizontal axes of a downhole instrument in a borehole. (The example assumes H1 is originally referenced as + south and H2 as + east.) The rotation of the instrument axes from true north can be determined by subtracting the azimuth of any shot relative to the sensors (as determined from particle velocity plots such as in Figure 3) from the azimuth of the shot relative to true north (as known from ship's navigation). Azimuth rotation for this example is 210°. (b). A plot showing an example of azimuth rotation vs. azimuth of shot from receiver for a series of shots fired at 30° intervals around the sensor depicted in (a). The rotation of the sensor axes indicated by arrivals from each shot is 210°.

Figure 5. A plot of azimuth rotation vs. shot azimuth from the OSS for the 23 shots used in the analysis. (a). The data have been fit by a sine curve restricted to one cycle in 360°. The three crossed out data points (shots 602, 617, and 618) were removed from consideration because of azimuth error introduced by basement topography (text and Figure 2). The 6.5° degree amplitude of the sine curve indicates that azimuth error is included in the azimuth rotation. (b). The amplitude of the sinusoidal curve has been reduced to nearly zero following relocation of the OSS by 513m to the west. The direction of relocation is dictated by the zero crossings of the sinusoidal curve (90° and 270°).

Figure 6. A depiction of azimuth error produced by inaccurate receiver location for 2 particular shot patterns. The inaccurate and corrected receiver locations are depicted with an arrow pointing toward the corrected receiver position. Shots in line with the inaccurate and corrected receiver

positions will have no azimuth error. Shots perpendicular to the line betwen corrected and inaccurate receiver positions will have maximum azimuth error. The maximum azimuth error for these shots is equal to the amplitude of the sinusoidal pattern (example in Figure 5a) produced by receiver mislocation in the azimuth rotation vs. azimuth data. Original and corrected positions for OSS-IV are shown in Figure 2.